A MODEL FOR MATRIX ACIDIZING OF LONG HORIZONTAL WELL IN CARBONATE RESERVOIRS

A Thesis

by

VARUN MISHRA

Submitted to the Office of Graduate Studies of
Texas A&M University
in partial fulfillment of the requirements for the degree of

MASTER OF SCIENCE

August 2007

Major Subject: Petroleum Engineering

A MODEL FOR MATRIX ACIDIZING OF LONG HORIZONTAL WELL IN CARBONATE RESERVOIRS

A Thesis

by

VARUN MISHRA

Submitted to the Office of Graduate Studies of
Texas A&M University
in partial fulfillment of the requirements for the degree of

MASTER OF SCIENCE

Approved by:

Chair of Committee,	Ding Zhu
Committee Members,	A. Daniel Hill
	P. Daripa
Head of Department,	Stephen A. Holditch

August 2007

Major Subject: Petroleum Engineering

ABSTRACT

A Model for Matrix Acidizing of Long Horizontal Well in Carbonate Reservoirs.

(August 2007)

Varun Mishra, B.Tech., Indian School of Mines

Chair of Advisory Committee: Dr. Ding Zhu

Horizontal wells are drilled to achieve improved reservoir coverage, high production rates, and to overcome water coning problems, etc. Many of these wells often produce at rates much below the expected production rates. Low productivity of horizontal wells is attributed to various factors such as drilling induced formation damage, high completion skins, and variable formation properties along the length of the wellbore as in the case of heterogeneous carbonate reservoirs. Matrix acidizing is used to overcome the formation damage by injecting the acid into the carbonate rock to improve well performance.

Designing the matrix acidizing treatments for horizontal wells is a challenging task because of the complex process. The estimation of acid distribution along wellbore is required to analyze that the zones needing stimulation are receiving enough acid. It is even more important in cases where the reservoir properties are varying along the length of the wellbore.

A model is developed in this study to simulate the placement of injected acid in a long horizontal well and to predict the subsequent effect of the acid in creating wormholes, overcoming damage effects, and stimulating productivity. The model tracks the interface between the acid and the completion fluid in the wellbore, models transient flow in the reservoir during acid injection, considers frictional effects in the tubulars, and predicts the depth of penetration of acid as a function of the acid volume and injection rate at all locations along the completion. A computer program is developed implementing the developed model. The program is used to simulate hypothetical examples of acid placement in a long horizontal section. A real field example of using the model to history match actual treatment data from a North Sea chalk well is demonstrated. The model will help to optimize acid stimulation in horizontal wells.

DEDICATION

To my parents and friends, the source of my inspiration.

ACKNOWLEDGMENTS

I would like to thank to my advisors, Dr. Ding Zhu and Dr. A. Daniel Hill, who guided me throughout the course of this research with extraordinary kindness and patience.

I would also like to thank the sponsors of the Middle East Carbonate Stimulation joint industry project at Texas A&M University for support of this work. Finally, thanks to Dr. Prabir Daripa, for his help and support for being a member of my committee.

TABLE OF CONTENTS

Page

ABSTRACT iii

DEDICATION iv

ACKNOWLEDGMENTS v

TABLE OF CONTENTS vi

LIST OF FIGURES viii

LIST OF TABLES x

CHAPTER

I INTRODUCTION 1

1.1 Background 1
1.2 Literature review 2
1.3 Objective and approach 4

II MATRIX ACIDIZING MODEL DEVELOPMENT 6

2.1 Wellbore flow model 7
2.1.1 Wellbore material balance 7
2.1.2 Wellbore pressure drop 8
2.2 Reservoir flow model 9
2.3 Model for tracking fluid interfaces 10
2.4 Wormhole model 11
2.4.1 Volumetric wormhole model 12
2.4.2 Buijse's semiempirical wormhole model 12
2.5 Skin and well completion model 15
2.5.1 Formation damage skin 16
2.5.2 Cased and perforated completions 18
2.5.3 Slotted liner completions 24
2.5.4 Partial penetration skin model 28
2.5.5 Solution of matrix acidizing model 31

III MATRIX ACIDIZING SIMULATOR 33

3.1 Matrix acidizing simulator 33
3.2 Simulator data files 34
3.2.1 Input data file 34
3.2.2 Output data files 35

CHAPTER Page

IV RESULTS 36
4.1 Hypothetical examples 36
4.1.1 Horizontal well with openhole completion 36
4.1.2 Horizontal well with cased-perforated completion 42
4.1.3 Horizontal well with slotted liner completion 46
4.1.4 Heterogeneity effect in horizontal well acidizing 49
4.2 Field study 53
V CONCLUSIONS 59
5.1 Conclusions 59
REFERENCES 60
NOMENCLATURE 62
APPENDIX A MATRIX ACIDIZING SIMULATOR 67
APPENDIX B MATRIX ACIDIZING SIMULATOR INPUT DATA FILE 76
VITA 79

LIST OF FIGURES

FIGURE Page

2.1 Schematic of a section of wellbore during an acidizing process 7
2.2 Interface movement inside the wellbore..... 11
2.3 Pore volume to breakthrough as a function of injection rate..... 14
2.4 Openhole horizontal well with formation damage around wellbore..... 17
2.5 Growth of wormhole from the tip of the perforation 18
2.6 Perforation skin components 19
2.7 Perforated well with deep penetration of damage..... 22
2.8 Perforated well with shallow penetration of damage 23
2.9 Geometric variables for slotted liner skin calculation..... 24
2.10 Flow geometries around a slotted liner 25
2.11 A section of partially completed vertical wellbore 28
2.12 Horizontal well partially open to the reservoir 29
2.13 Ellipsoidal flow geometry..... 30
4.1 Acid coverage over the entire length of wellbore 39
4.2 Wormhole length distributions at different times 39
4.3 Acid placement profiles for 200 and 500 bbls of acid 40
4.4 Acid placement profiles for different values of PV_{bt}..... 40
4.5 Pressure responses during acid injection..... 41
4.6 PV_{bt} versus V_i during simulation using Buijse Model with $PV_{bt\text{-}opt}$=1.5 41
4.7 Comparison of wormhole distributions from volumetric and Buijse's models. 42
4.8 Distribution of perforation length along the wellbore..... 44
4.9 Evolution of skin with time during acid injection..... 44
4.10 Acid coverage in cased-perforated completion case 45
4.11 Distribution of wormholes in cased-perforated completion case..... 45
4.12 Comparison of acid coverage in uniform and non-uniform perforation length distribution 46
4.13 Distribution of wormhole length in slotted liner completion 48

FIGURE Page

4.14 Distribution of skin in slotted liner completion 48
4.15 Distribution of initial damage along the length of wellbore 50
4.16 Distribution of permeability along the length of wellbore 50
4.17 Acid coverage along the length of wellbore 51
4.18 Injectivity index during the acid injection 52
4.19 Local skin factors along the wellbore at the end of simulation 52
4.20 Selective stimulation for each perforated zone using straddle packers and perforated coiled tubing 53
4.21 Pressure response of downhole gauges 54
4.22 Rate schedule for North Sea field well acid treatment 54
4.23 History match of treatment pressure 56
4.24 Acid placement for North Sea field well 57
A.1 A schematic of segmented wellbore 70
A.2 A flow chart for matrix acidizing simulator 73

LIST OF TABLES

TABLE Page

2.1 Correlation constant, a_m 21

2.2 Correlation constants, b_m and c_m 21

2.3 Correlation constants, d_m e_m, f_m and g_m 21

3.1 Matrix acidizing simulator data files 34

4.1 Data for acid injection into horizontal well with openhole completion 37

4.2 Data for acid injection into horizontal well with cased-perforated completion 43

4.3 Data for acid injection into a horizontal well with slotted liner completion 47

4.4 Data for acid injection into a horizontal well with thief zones 49

4.5 Input data for North Sea field well 55

CHAPTER I

INTRODUCTION

1.1 Background

Starting in the 1980s, horizontal wells began capturing an ever-increasing share of hydrocarbon production. They proved to be excellent producers for thin (h<50 ft) reservoirs or for thicker reservoirs with good vertical permeability, k_V.

Horizontal wells are drilled to achieve improved reservoir coverage, high production rates, and to overcome water coning problems etc. Many of these wells often produce at a rate below the expected production rates. Low productivity of horizontal wells is attributed to various factors such as drilling induced formation damage, high completion skins, and variable formation properties along the length of the wellbore as in the case of heterogeneous carbonate reservoirs.

Positive skin effects are created by "mechanical" causes such as partial completion, by altering the relative permeability of original fluid, by turbulence, and by damage to the original permeability. Formation damage in horizontal wells is unavoidable due to longer exposure time of wellbore to the drilling and completion fluid. The fine particles contained in drilling fluid migrate inside the formation rock and plug the pore spaces which results in reduction of formation permeability[1].

Investigations in the past have shown that positive skins are detrimental to the performance of horizontal wells. Various completion techniques are also adopted for horizontal wells such as openhole completions, cased perforated completions, and slotted liner completions. These completions may also contribute to the positive skin factors resulting in much higher skin values than damage skin alone.

Matrix acidizing is a techniques to stimulate the well by removing near wellbore damage. In sandstone reservoirs, matrix acidizing is often considered for many people as risky to

---

This thesis follows the style of *SPE Production and Operations*.

undertake due primarily to heterogeneous nature of formation minerals and an appreciable degree of unpredictability of their response to acid formulations[2]; however, in carbonate reservoirs it is a relatively simple stimulation technique that has became one of the most cost-effective method to improve significantly the well productivity and hence the hydrocarbons recovery. The success rate of the treatments in carbonate reservoirs is 30%-50%.

During matrix acidizing treatments the acid is injected at pressures below the fracture pressure to avoid fractures being created during the treatments. The acid reacts within a few inches from wellbore in sandstones and a few feet in carbonates[1]. In carbonate formations matrix acidizing is used as a tool to overcome the formation damage by injecting the acid into the carbonate rock which results in formation of wormholes.

Acid stimulation is a cost effective method to enhance the productivity of horizontal wells in carbonate reservoirs. Acid can be injected by bullheading down the production tubing, through coiled tubing, or into intervals by isolating packers, or injection from acid jetting tools. Effective stimulation requires that sufficient acid volume be placed in all desired zones.

1.2 Literature review

Designing the matrix acidizing treatments for horizontal wells is a challenging task because of the complex processes involved. The acid distribution along the wellbore is hard to predict and it becomes more difficult in case of varying reservoir properties along the wellbore.

Jones and Davies[3] made an attempt to quantify the acid placement in horizontal wells. According to them the key to the treatment success is maximizing the acid coverage over the length of the wellbore. The model presented was for barefoot completions in sandstone formations and the simulator used a pseudo-steady state reservoir model. They concluded that variation in reservoir properties along the treatment interval significantly impacts the acid placement over the wellbore length. The need to include wellbore phenomena was also emphasized in their work.

Buijse and Glasbergen[4] used a placement simulator to predict the zonal coverage of stimulation fluids in long vertical wellbore. The fluid placement simulator was based on the model described by Davies and Jones. The model assumes a piston type displacement between various fluids in the wellbore. They used different diversion methods in simulating the stimulation treatments in long intervals. Based on the simulation results it was concluded that the fluid distribution in heterogeneous formations such as carbonate reservoirs can only be understood to its full extent by using a numerical simulator. To evaluate a past design or to optimize a future acidizing treatment a fluid placement simulator is essential. Their conclusion also holds true for long horizontal wells placed in carbonate reservoirs. Carbonate reservoirs are heterogeneous in nature and horizontal wells drilled in carbonate reservoirs most likely have non-uniform formation properties along the wellbore length. During acid treatments of these wells heterogeneity causes difficulty in predicting the distribution of acid along the entire wellbore length. So a fluid placement simulator is necessary to understand the resulting fluid distribution thus optimizing the future treatments.

Eckerfield et al.[5] concluded in their work that movement of interfaces formed between acid and completion fluids is significantly affected by uneven reservoir flow distribution, which ultimately leads to nonuniform volume of acid injected into the formation. Wellbore hydraulics was found to have much less impact because of the small wellbore volume relative to the volume of acid injected.

Gdanski[6] described recent advances in carbonate stimulation stating that zonal coverage of long carbonate sections remains a challenge and most of the acidizing treatments are designed on the basis of past experience.

A study was conducted by Bazin et al.[7] to optimize the strategy for matrix treatment of horizontal drains in carbonate reservoirs. It was concluded that there should always be a well defined strategy for acidizing treatments of horizontal wells depending on the reservoir characteristics and no “rule of thumb” should be used else it may results in poor stimulation.

The acid placement techniques also play an important role in effective stimulation of the horizontal wells. Mitchell et al.[8] compared two acid placement techniques i.e. bullheading and coiled tubing injection used in offshore fields of Java Sea. The authors concluded in their work that coiled tubing stimulation provides a greater increase in productivity index which sustains for longer period of time. It was found that the coiled tubing enable stimulation fluids to be placed where they are needed. The additional cost of using the coiled tubing can be offset by the incremental production but offshore operating conditions limit the use of coiled tubing. In such cases injection through bullheading was found as an inexpensive way to stimulate the wells.

1.3 Objective and approach

The presented research project aims to develop an acid stimulation model to study the acid distribution and evolution of skin during acidizing treatments in the horizontal wells in carbonate reservoirs. This model considers the frictional pressure drop along the wellbore. It tracks interfaces between various injected fluids and models the transient flow response of the reservoir. The model couples a wellbore flow model, an interface tracking model, a wormhole model, a skin evolution model, and a transient reservoir inflow model. The model predicts the bottomhole pressure response during an acid treatment, the distribution of acid along the treated section, and the resulting skin factor during stimulation. This model is capable of handling the variable formation properties along the wellbore such as porosity, permeability, etc.

The formulation of the various model equations is presented in Chapter II. The model couples several processes together. Each process is described separately in this chapter. A method to solve the model equations is also presented in this chapter.

A computer program is developed incorporating the new model which can be used to design and evaluate the acidizing treatments in long horizontal wells. Using the developed computer program an analysis of the evolution of skin and acid coverage will be performed for past as well as future treatments. In Chapter III, the program flow chart and information about input and output data files are presented.

In Chapter IV, results of hypothetical cases and actual field studies are presented. One hypothetical case is presented assuming uniform distribution of reservoir properties along the wellbore. The effect of variable formation properties is also studied using the developed program. It was found that their effect is significant on the acid distribution along the wellbore.

A field case is presented in which a history match of observed pressure data and simulated pressure data was done by varying parameters which influence the treatment. The analysis of acid treatments in small wellbore section is done using the developed model. The impact of partial penetration skin on acid treatment response is investigated. The lessons learned by evaluating the past treatments might pave a way to optimize our future treatments to achieve higher productivities from the horizontal wells.

CHAPTER II

MATRIX ACIDIZING MODEL DEVELOPMENT

In this chapter, an acidizing model for horizontal well is presented. In a typical matrix acidizing process the acid is injected into the formation through production tubing, coiled tubing, or drill pipe. The acid displaces the wellbore fluid, forming interfaces between different fluids. The acid flows into the formation and creates wormholes in the reservoir rock, increasing the injectivity of the contacted portions of the formation. The effect of acid on the formation injectivity at any location along the well is accounted for with a local skin factor that is changing in response to the acid injected at that point. Local injectivity is simultaneously affected by the transient nature of the process as injection of any fluid causes a pressure build up in the porous medium. The transient pressure build up due to the injection and the acid stimulation that is increasing injectivity are competing effects that must both be considered to properly predict acid placement.

To simulate the acidizing process above, all of the processes are studied separately. These include a wellbore model which handles the pressure drop and material balance in the wellbore; an interface tracking model to predict the movement of interfaces between different fluids in the wellbore; a transient reservoir flow model; a skin factor model accounting for partial penetration and well completion effects; and, an acid stimulation model that predicts wormhole growth and the effects these have on local injectivity. Each model is discussed in this chapter separately.

The coupled model allows for an arbitrary distribution of perforations along the completion, initial damage, reservoir permeability, and a user-specified acid treatment schedule. The model predicts the acid coverage and wormhole penetration as functions of position along the wellbore and injection time. A solution scheme is presented to simulate the bottomhole pressure response during the treatment. This response can be matched with the actual pressure response during the treatment.

2.1 Wellbore flow model

The wellbore flow model is developed based on wellbore material balance and wellbore pressure drop calculations. The fluids injected during the acid injection process are mostly incompressible so single phase incompressible flow in the wellbore is assumed to develop these equations.

2.1.1 Wellbore material balance

Figure 2.1 shows a schematic of a horizontal wellbore during an acid injection process. Single phase (liquid) flow through a reservoir injected by a fully penetrating horizontal well is considered. It is also assumed that all of the reservoir flow is perpendicular to the wellbore. p_w is wellbore pressure at any point in the wellbore, q_w is the flow rate in the wellbore, and q_R is specific reservoir outflow i.e. per unit length. Since the flow rate changes along the wellbore is caused by the fluid flowing into the reservoir, by material balance, we have,

$$\frac{\partial q_w}{\partial x} = -q_R \tag{2.1}$$

Equation 2.1 states that the specific reservoir outflow, q_R (bbl/ft) should be equal to the decrease in wellbore flow rate per unit length, q_w (bbl).

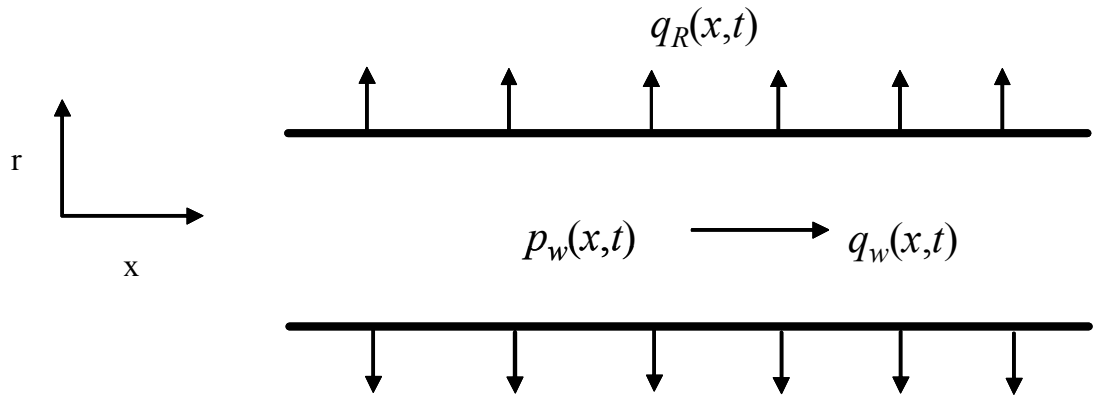

Figure 2.1 Schematic of a section of wellbore during an acidizing process

2.1.2 Wellbore pressure drop

If steady state flow exists in a horizontal pipe and fluid has a constant density, then friction pressure drop is obtained from the Fanning equation[1],

$$\Delta P_F = \frac{2 f_f \rho u^2 L_{pipe}}{g_c d} \tag{2.2}$$

In the differential form the above equation can be written as,

$$\frac{\partial p_w}{\partial x} = -\frac{2 f_f \rho u^2}{g_c d} \tag{2.3}$$

In the above equation f_f is defined as the Fanning friction factor, and u is defined as the fluid velocity.

$$u = \frac{q_w}{A} \tag{2.4}$$

Equation 2.4 relates the fluid velocity with the flow rate; where A is the cross-section area of the pipe and q_w is the fluid flow rate in the pipe. Eq. 2.3 is rearranged for the oil field units as;

$$\frac{\partial p_w}{\partial x} = -1.525 f_f \frac{\rho q_w^2}{d^5} \tag{2.5}$$

Where p_w is in psi, x is in ft, ρ is in lb_m/ft^3, d is in inches, and q_w is in bpm.

Equation 2.5 provides the equation for pressure drop in a horizontal wellbore during the acid injection process. This equation will be coupled with the other system equations to setup the matrix acidizing model.

The Fanning Friction factor depends on the Reynolds number, N_{RE}, and pipe roughness, ε. Fluid flow is characterized as laminar or turbulent, depending on the value of the Reynolds number, N_{RE}, defined for a circular pipe as

$$N_{\mathrm{Re}} = \frac{du\rho}{\mu} \tag{2.6}$$

Consistent units must be used in the evaluation of the Reynolds number so that N_{Re} is dimensionless. Laminar flow exists within the pipe when Reynolds number is less than 2000. For turbulent flow, Reynolds number is greater than 4000. The flow is called transitional, if Reynolds number lies between 2000 and 4000.

The Fanning friction factor is most commonly obtained from the Moody friction factor chart. But for computational purposes the following equations are used to determine the friction factor. In laminar flow, the friction factor is inversely related to the Reynolds number as;

$$f_f = \frac{16}{N_{\mathrm{Re}}} \tag{2.7}$$

For turbulent flow, an explicit equation for the friction factor is the Chen equation[1];

$$\frac{1}{\sqrt{f_f}} = -4\log_{10}\left\{\frac{\varepsilon}{3.7065} - \frac{5.0452}{N_{\mathrm{Re}}}\left[\frac{\varepsilon^{1.1098}}{2.8257} + \left(\frac{7.149}{N_{\mathrm{Re}}}\right)^{0.8981}\right]\right\} \tag{2.8}$$

Parameter obtained from the pressure drop equation, i.e. p_w or q_w, from the wellbore model will be used in the reservoir flow model.

2.2 Reservoir flow model

During the acidizing process, the wellbore rate and the reservoir inflow at any location are changing with time so transient effects are occurring in the reservoir. With the superposition principle the outflow estimation to include the transient effects during acid injection process can be estimated as[9];

$$-\frac{2\pi kl}{\mu}(p_R - p_w) = \sum_{j=1}^{n} \Delta q_j \left[p_D(t_n - t_{j-1})_D\right] + q_n s_n \tag{2.9}$$

Where:

$$\Delta q_j = q_j - q_{j-1} \tag{2.10}$$

$$t_D = \frac{4.395\times10^{-6} kt}{\phi\mu c_t {r_w}^2} \tag{2.11}$$

$$p_D \approx \frac{1}{2}(\ln t_D + 0.80907) \tag{2.12}$$

Equation 2.9 provides the wellbore pressure (p_w) at n^{th} time step when the reservoir inflow rate, q, is varying with time. p_R is defined as initial reservoir pressure when there was no flow from the wellbore to the reservoir. The parameter s in the Eq. 2.9 represents the local skin factor and it changes continuously with acid injection. Reservoir permeability, porosity, compressibility and injected fluid viscosity are defined as k, Φ, c_t, and μ, respectively. r_w is wellbore radius. All of the variables used in the equations are in oil field units as defined in the appendix.

Once the reservoir outflow and transient pressure response is obtained, it is required to calculate the volume of specific fluid injected into the formation. As during injection, multiple interfaces may exist, an interface tracking model is used to calculate the position of an interface. Once locations of the interfaces are obtained the volume injected behind the fronts are to be calculated.

2.3 Model for tracking fluid interfaces

A model to track the interfaces created between various injected fluids was presented by Eckerfield et al.[5] This acid placement model will use a discretized solution approach which is integrated with the reservoir flow, wormhole, and skin models. Fig. 2.2 depicts a part of the wellbore where the interface created between injected acid and wellbore fluid is traveling to the right. The velocity of an interface located at x_{int} is simply,

$$\frac{dx_{\text{int}}}{dt} = \left.\frac{q_w}{A}\right|_{x=x_{\text{int}}} \tag{2.13}$$

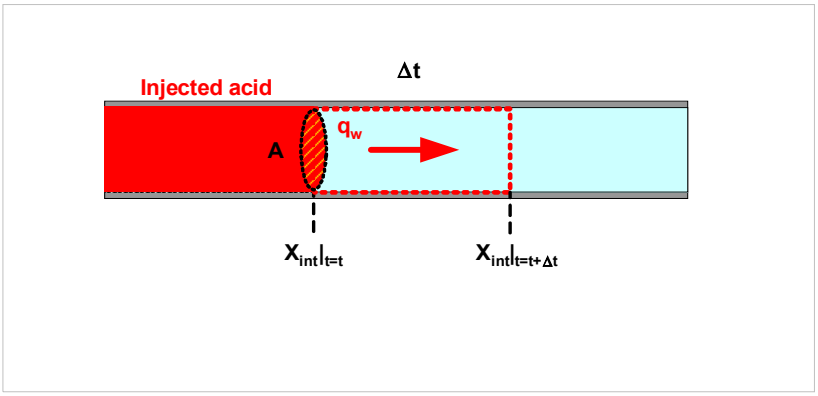

Figure 2.2 Interface movement inside the wellbore

In discrete form the location of interface at time (t+Δt) can be written as

$$x_{\text{int}}\big|_{t=t+\Delta t} = x_{\text{int}}\big|_{t=t} + \left.\frac{q_w}{A}\right|_{x=x_{\text{int}}} \Delta t \tag{2.14}$$

where A is the cross-sectional area of flow in the pipe. Eq. 2.14 is solved by discretizing the wellbore into small segments and assuming constant q_w over each segment.

Once the interfaces and outflows in the wellbore parts are estimated it is necessary to get the growth of wormhole during that injection time. A wormhole model is applied with injection volume or rate as input to get the wormhole growth. Length of wormhole is calculated by integrating growth in every small time step.

2.4 Wormhole model

When the acid (HCl) is injected into carbonate rocks, due to very high surface reaction rates, mass transfer limits the overall reaction rate, leading to highly nonuniform dissolution pattern, and few large channels are formed known as wormholes. Wormholes bypass the damaged near wellbore region and improve the flow conditions. Creation of wormholes and optimization of the wormhole length are main goals in acid treatment design. It is important to gain an understanding of parameters that affect the wormhole growth. Structure of these wormholes depends on many factors such as flow geometry, injection rate, reaction kinetics, and mass transfer rate.

Fredd and Miller[10] presented an excellent review of the different models that have been presented in the past. The authors work was focused on validating the wormhole models with the laboratory data from linear flow experiments. Two models of the wormholing process will be implemented in this work.

2.4.1 Volumetric wormhole model

The volumetric model[1, 11] is based on the assumption that a constant fraction of the rock volume is dissolved in the region penetrated by wormholes. For radial flow, the volumetric model is

$$r_{wh} = \sqrt{r_w^{\,2} + \frac{V/l}{\pi\phi PV_{bt}}} \tag{2.15}$$

where r_{wh} is distance of wormhole tip from the wellbore center, V/l is the volume of acid injected per unit length of formation. When only a few wormholes are formed, a small fraction of the rock is dissolved; more branched wormhole structures dissolve larger fractions of the matrix. The key parameter in this model is PV_{bt}, the number of pore volumes of acid needed to propagate a wormhole through a certain distance. The PV_{bt} can vary in a large range, depending mainly on the rock mineralogy.

If the PV_{bt} is obtained from a radial core flood, it should predict wormhole propagation in a well treatment where the flow is radial, at least for wormhole propagation to the same distance as that tested in the core flood. If a linear core flood is used to measure PV_{bt}, the wormhole propagation in radial flow will probably be somewhat overestimated.

2.4.2 Buijse's semiempirical wormhole model

An improved empirical model of the wormholing process is presented by Buijse and Glasbergen[12]. The authors adopted an alternative approach and described the wormhole growth by a simple model. In this model the growth rate of the wormhole front is modeled as a function of acid injection rate which is in fact related to acid velocity in the pores. The effect of acid velocity is more significant in case of perforated completions. This model is semiempirical as the effect of parameters such as temperature, acid

concentration; permeability and mineralogy are not modeled explicitly. The effect of these parameters is included in the model in two constants, W_{eff} and W_B. The value of these constants can be calculated from the results of a core flow experiment in the laboratory or by fitting the model to field results.

According to this model, in radial geometry, the wormhole growth rate depends on the injection rate and also on the position of the wormhole front in the formation. The interstitial fluid velocity is defined as,

$$V_i = \frac{Q}{2\pi r l \phi} \tag{2.16}$$

where r is the distance of the wormhole tip from the center of the wellbore. Eq. 2.16 explains that how the interstitial fluid velocity and the wormhole length are inversely related. The wormhole velocity is can be also calculated as,

$$V_{wh} = W_{eff} . V_i^{2/3} . B \tag{2.17}$$

where parameter W_{eff} , W_B , and B can be calculated by using Eqs. 2.18, 2.19, and 2.20 as,

$$B = \left(1 - \exp\left(-W_B . V_i^2\right)\right)^2 \tag{2.18}$$

$$Weff = \frac{V_{i-opt}^{1/3}}{PV_{bt-opt}} \tag{2.19}$$

$$W_B = \frac{4}{V_{i-opt}^2} \tag{2.20}$$

Ideally the constants W_{eff} and W_B are calculated from the results of radial core flow tests. The radial core flow tests are difficult and expensive to perform and sometimes there are no data available. In that case these constants can be determined using the data of linear core flow tests in Eqs. 2.19 and 2.20. The optimum values of fluid velocity, $V_{i\text{-}opt}$, and break through pore volume, $PV_{bt\text{-}opt}$, can be obtained from the liner core flow tests.

Once the wormhole velocity is obtained, the growth of the wormhole can be obtained by discretizing the time domain as the wormhole velocity depends on the interstitial fluid velocity, which in turn depends on the distance of wormhole tip from the center. In this model, the wormhole propagation rate varies with the acid flux in a manner based on the commonly observed "optimal flux" behavior. The optimal acid flux and the optimal PV_{bt} are based on laboratory tests.

The authors gathered the data for core flow tests results from in-house experiments and from literature. A log-log plot of this data is shown in Fig. 2.3 where the pore volumes to breakthrough are plotted as a function of injection rate. The curves are fitted to the measured data points using the equation below,

$$PV_{bt} = \frac{V_i}{V_{wh}} = \frac{V_i^{1/3}}{W_{eff} B} \tag{2.21}$$

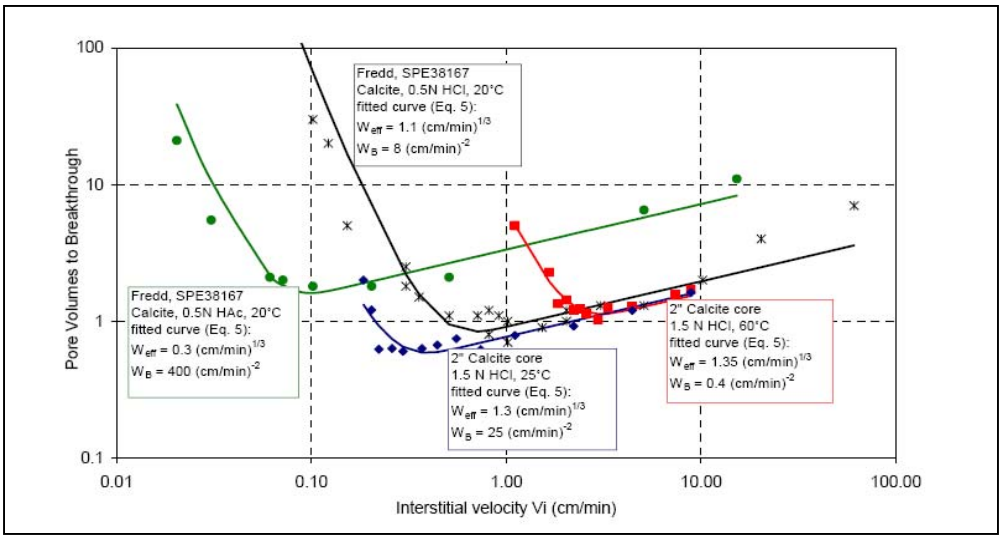

Figure 2.3 Pore volume to breakthrough as a function of injection rate[12]

Equation 2.21 explains that with changing interstitial fluid velocity, i.e. V_i, the pore volumes for breakthrough changes and it does not remain constant during the injection as in volumetric wormhole model. It can be seen from the Fig. 2.3 that on this log-log plot, there exists an optimum value of PV_{bt} and V_i , which are termed as $PV_{bt\text{-}opt}$ and

$V_{i\text{-}opt}$. During the acid injection treatments, if the interstitial fluid velocity falls below the optimum i.e. $V_{i\text{-}opt}$, the PV_{bt} increases with the decreasing V_i and the face dissolution of carbonate rock occurs. If the acid is injected at the rate so that interstitial fluid velocity remains above the optimum, the PV_{bt} decreases with the decreasing V_i. So at high interstitial fluid velocities, B approaches to 1 and Eq. 2.21 holds true,

$$PV_{bt} \propto V_i^{1/3}$$
$$V_{wh} \propto V_i^{2/3} \tag{2.22}$$

During the acid injection in field conditions, the Buijse's model recommends the acid injection rate to be maintained above the optimum injection rate but staying below the fracturing pressure. Both of the models, the volumetric and the Buijse's model of wormhole propagation are to be implemented in the acidizing simulator. If the PV_{bt} input to the volumetric model is close to the average value of PV_{bt} (as it changes throughout the injection) determined by the Buijse's model at the acid flux occurring in the simulated acid treatment, the results from these two models should be similar.

The wormhole model provides the length of wormhole as an input to the skin model, which then calculates the skin factor. Skin factors are updated at every time step.

2.5 Skin and well completion model

The horizontal wells drilled in carbonate reservoirs can be completed with several completion techniques. The common completion types are openhole completions, cased and perforated completions and slotted liner completions. Positive skin factors are found in openhole completions mostly due to formation damage. The other two completion techniques might introduce positive completions skin factors along with the formation damage skin.

The changing injectivity during acid injection is accounted for with a local skin factor, $s(x)$, which includes the effects of the completion, possible formation damage, and stimulation with a positive value for completion, and a negative value for stimulation. The effects of the completion, formation damage, and stimulation are all coupled.

During the matrix acidization process the wormholes are created and propagate into the formation. The propagation of wormholes into the formation lowers the skin and enhances the productivity of the well. The evolution of skin factors for each type of completions are discussed in separate sections.

In addition, injectivity of individual zones along a long horizontal well are affected by a partial penetration effect which can be treated as a skin effect. This partial penetration effect is also described in later section.

2.5.1 Formation damage skin

Formation damage occurs due to the reduction in original permeability of the rock. The original permeability can be altered due to fines migration from drilling and completion fluid, or relative permeability alteration etc. In openhole completions, the damage skin can cause sufficient pressure drop to reduce the production rate. In openhole completions the wellbore have direct contact with the formation and whole cylindrical surface area of wellbore is open to flow.

Openhole completions are the simplest and the cheapest. Their use is restricted to reservoirs formed of competent rock that is sufficiently strong to withstand collapsing stresses. Openhole completions provide the maximum flexibility for future well modification. For example, it is possible, at a later stage, to insert a liner with external casing packers or even to convert an open hole well to a fully cemented completion.

Figure 2.4 shows an openhole completion of a horizontal well with formation damage in the near wellbore region. r_d is defined as the damaged radius beyond the wellbore and r_{wh} is defined as the length of the wormholes. Ideally these two parameters vary with the length and may have a nonuniform distribution along the length of the wellbore.

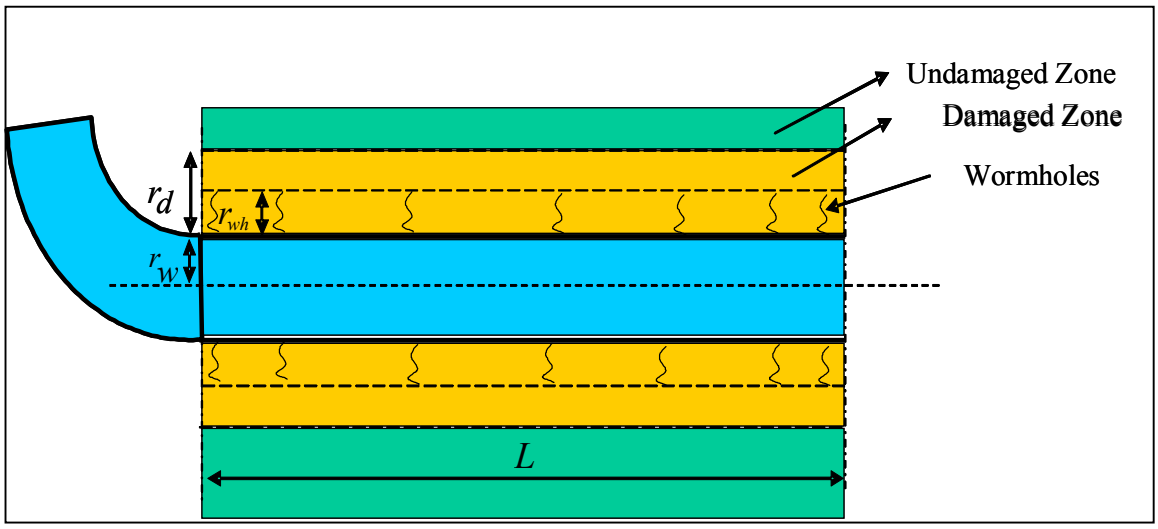

Figure 2.4 Openhole horizontal well with formation damage around wellbore

Under the assumption that the pressure drop in the wormhole is small, these wormholes can be considered as infinite conductivity channels. The local skin factor at any general point x along the wellbore can be achieved by applying the Hawkins formula for skin at that point.[1]

For $r_{wh}<r_d$:

$$s(x)=\frac{k}{k_d(x)}\ln\left(\frac{r_d(x)}{r_{wh}(x)}\right)-\ln\left(\frac{r_d(x)}{r_w}\right) \tag{2.23}$$

And for $r_{wh}>r_d$:

$$s(x)=-\ln\left(\frac{r_{wh}(x)}{r_w}\right) \tag{2.24}$$

where r_{wh} is radius of region penetrated by wormholes at that particular point, which is to be calculated from the wormhole model.

It is evident from the above equations that as the wormholes grow longer the skin factor decreases. The skin factor needs to be updated at each time step after calculating the wormhole length at the end of time step.

2.5.2 Cased and perforated completions

Cased and perforated completions are also a commonly used method for horizontal well completion. Perforation is the communication tunnel extending beyond casings or liners into the reservoir formation, through which oil or gas is produced. In most cases, a high penetration is desirable to create effective flow communication to the part of the formation that has not been damaged by the drilling or completion processes.

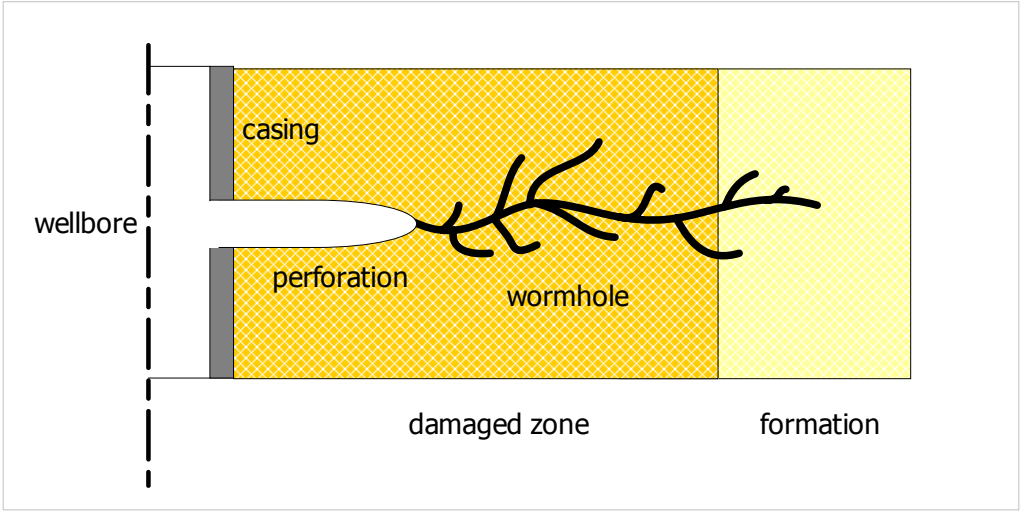

Figure 2.5 Growth of wormhole from the tip of the perforation

For a cased, perforated completion, the perforation skin factor model of Furui et al.[13] is used. The model assumes that wormholes propagating from the tips of perforations can be considered as extensions of the effective lengths of the perforations as in Fig. 2.5.

On the basis of above assumption the effective length of perforation at any time step can be written by Eq. 2.25,

$$l_{p,eff} = l_p + r_{wh} \tag{2.25}$$

where l_p is perforation length which remains constant over time, $l_{p,eff}$ is effective perforation length at certain time, and r_{wh} is length of wormhole at that time.

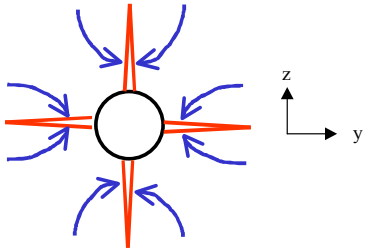

(a) 2-D (y-z) convergence s_{2D}

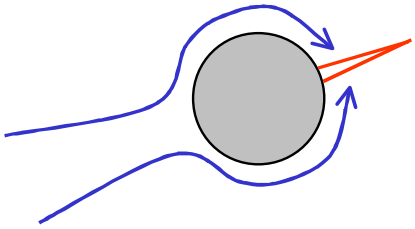

(b) Wellbore blockage s_{wb}

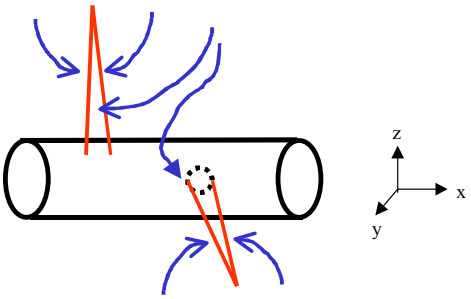

(c) 3-D convergence s_{3D}

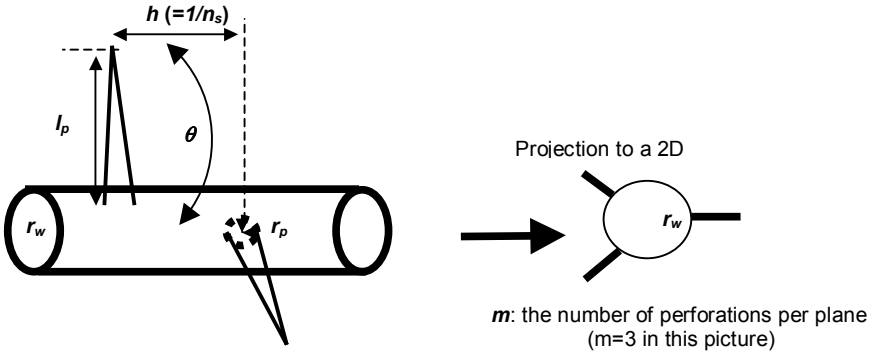

Figure 2.6 Perforation skin components

The perforation skin can be divided into three components (Fig. 2.6); the 2D plane flow skin, s_{2D}; the wellbore blockage skin, s_{wb}; and the 3D convergence skin factor, s_{3D}. The total perforation skin factor is then given by Eq. 2.26,

$$s_p = s_{2D} + s_{wb} + s_{3D} \tag{2.26}$$

s_{2D} is a skin factor that accounts for flow in the *y-z* plane without the existence of the wellbore. This skin factor can be negative or positive depending on the perforation conditions such as perforation phasing, perforation length and wellbore radius. For an isotropic formation,

$$s_{2D} = a_m \ln\left(\frac{4}{l_{pD}}\right) + (1 - a_m)\ln\left(\frac{1}{1 + l_{pD}}\right) \tag{2.27}$$

where l_{pD} is the dimensionless perforation length defined by

$$l_{pD} = l_p / r_w \tag{2.28}$$

s_{wb} is also estimated for the 2D plane flow geometry. The wellbore blockage skin correlation equation is empirically derived based on the FEM simulation results. For an isotropic formation,

$$s_{wb} = b_m \ln\{c_m / l_{pD} + \exp[-c_m / l_{pD}]\} \tag{2.29}$$

The numerical values of a_m, b_m and c_m given by Tables 2.1, and 2.2 respectively.

For low perforation shot densities, the flow geometry around a perforation becomes extremely complicated. According to Karakas & Tariq's work[14], the 3D convergence skin factor can be given by;

$$s_{3D} = 10^{\beta_1} h_D^{\beta_2 - 1} r_{pD}^{\beta_2} \tag{2.30}$$

$$\beta_1 = d_m \log r_{pD} + e_m \tag{2.31}$$

$$\beta_2 = f_m r_{pD} + g_m \tag{2.32}$$

$$h_D = \frac{h}{l_p} \tag{2.33}$$

$$r_{pD} = \frac{r_p}{h} \tag{2.34}$$

The numerical values of d_m, e_m, f_m, and g_m presented in Karakas and Tariq's paper[14], and are given by Table 2.3. These equations can be used to estimate the perforation skin factor for most practical ranges of system parameters ($h_D \leq 10$ and $r_{pD} \geq 0.01$).

Table 2.1 Correlation constant, a_m

m	a_m
1	1.00
2	0.45
3	0.29
4	0.19
∞	0.00

Table 2.2 Correlation constants, b_m, and c_m

m	b_m	c_m
1	0.90	2.0
2	0.45	0.6
3	0.20	0.5
4	0.19	0.3
∞	0.00	0.00

Table 2.3 Correlation constants, d_m, e_m, f_m, and g_m

m	d_m	e_m	f_m	g_m
1	-2.091	0.0453	5.1313	1.8672
2	-2.025	0.0943	3.0373	1.8115
3	-2.018	0.0634	1.6136	1.7770
4	-1.905	0.1038	1.5674	1.6935

The extension of the perforation skin model to account for formation damage and crushed zone effects is necessary. The reduced permeability can enhance the perforation skin depending on the length of perforations. If the perforation length is smaller than the damage radius, as shown in Fig. 2.7, the total skin can be expressed by,

$$s_t = s + (k/k_d)s_p \tag{2.35}$$

Where s is skin caused by formation damage alone,

$$s = (k/k_d - 1)\ln(r_d/r_w) \tag{2.36}$$

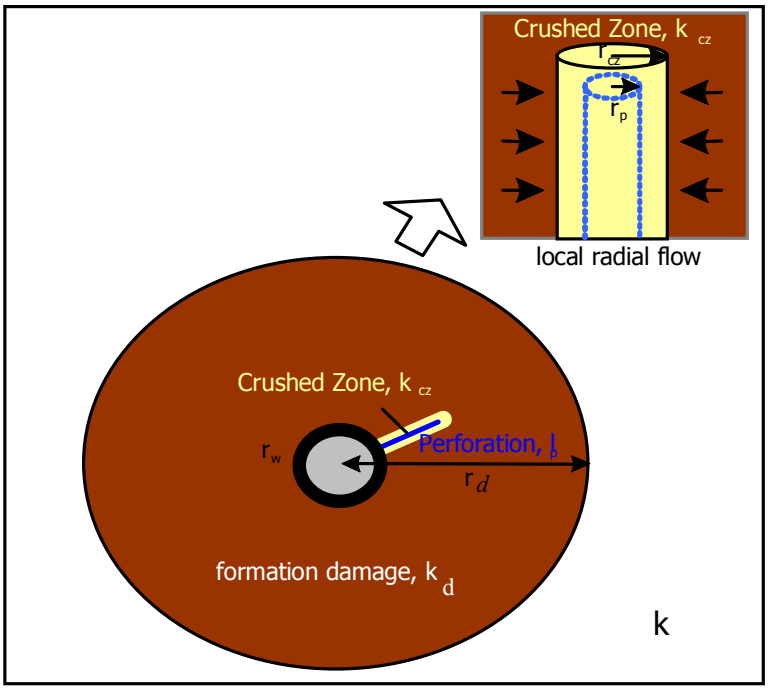

Figure 2.7 Perforated well with deep penetration of damage

As discussed by many authors, the permeability damage around the perforations from rock compaction can significantly impair well productivity. Assuming radial flow around the perforations and neglecting wellbore effects, the additional pressure drop caused by the crushed zone can be taken into account by the following equation;

$$s_t = s + \frac{k}{k_d}s_p + h_D\left(\frac{k}{k_{cz}} - \frac{k}{k_d}\right)\ln\left(\frac{r_{cz}}{r_p}\right) \tag{2.37}$$

For perforations extending beyond the damage zone (Fig. 2.8), the effect of formation damage is relatively smaller than that obtained by Eq. 2.37. The perforations create flow paths through the damaged zone for flow to reach the wellbore without substantial pressure drops. However, the flow concentration around the tip of the perforations will increase and results in additional pressure drop. As Karakas and Tariq proposed, the equivalent flow system can be obtained by simply replacing the perforation length and the wellbore radius by $l_{p,eff}$ and $r_{w,eff}$

$$l_{p,eff} = l_p - [1-(k_d / k)]l_{ps} \tag{2.38}$$

$$r_{w,eff} = r_w + [1-(k_d / k)]l_{ps} \tag{2.39}$$

where l_{ps} is the damage length covering over a perforation. Including the crushed zone effect, a skin equation for perforations outside the damage zone can be presented by

$$s_t = s_p + h_D\left(\frac{k}{k_{cz}} - 1\right)\ln\left(\frac{r_{cz}}{r_p}\right) \tag{2.40}$$

s_p has to be calculated using $l_{p,eff}$ and $r_{w,eff}$ and it should include the formation damage.

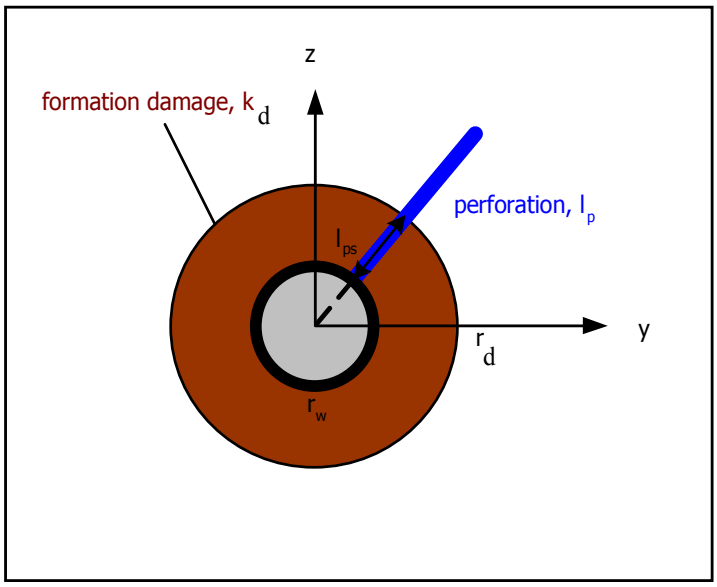

Figure 2.8 Perforated well with shallow penetration of damage

2.5.3 Slotted liner completions

A slotted liner has numerous long and narrow openings (slots) which are milled into the base pipe to allow fluids to flow into the liner. Slot style is characterized by the arrangement of the slots around the circumference of the liner (Fig. 2.9).

Furui et al. [13] developed a skin equation for slotted liners which accounts mainly for the flow convergence to the slots, the slot plugging, effects of formation damage and the interactions among these effects. In the presence of formation damage around the well the overall skin is magnified.

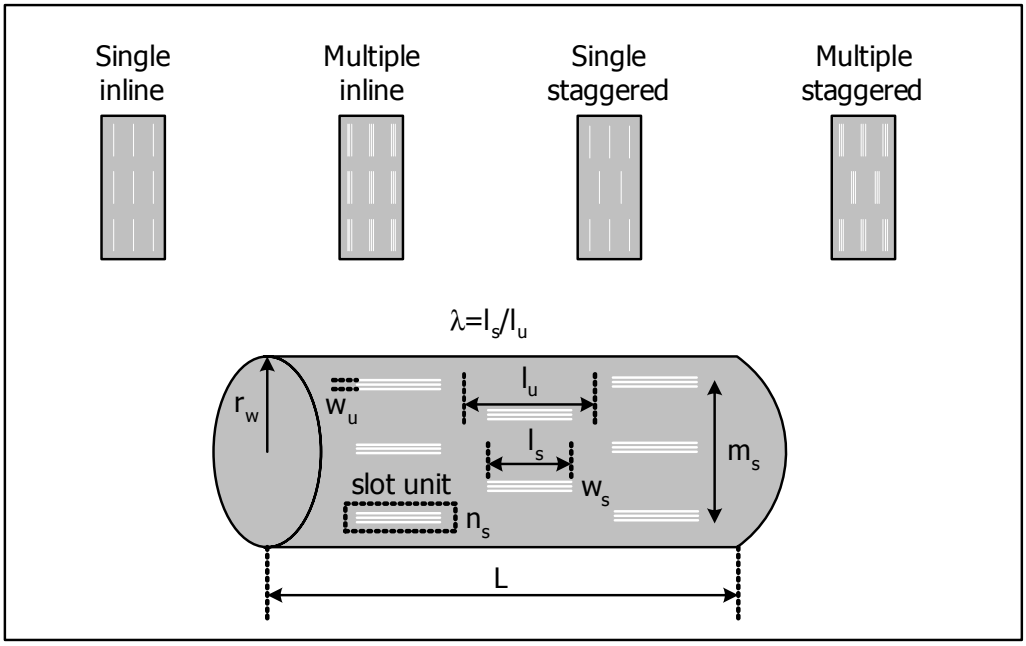

Figure 2.9 Geometric variables for slotted liner skin calculation[13]

In our case it is assumed that there is no turbulent flow inside the formation which reduces the rate dependent skin to zero. The skin of a slotted liner is given by,

$$s_{SL} = s_{SL,l} + s_{SL,r} \tag{2.41}$$

The subscript, *l* and *r*, denote the linear flow inside the slots and the radial flow outside the liner. The skin for the linear flow geometry is assumed to be zero for unplugged slots ($s_{SL,l}$=0). The rate-independent skin, $s_{SL,r}$, for the radial flow geometry is to be calculated by consideration of each flow regime.

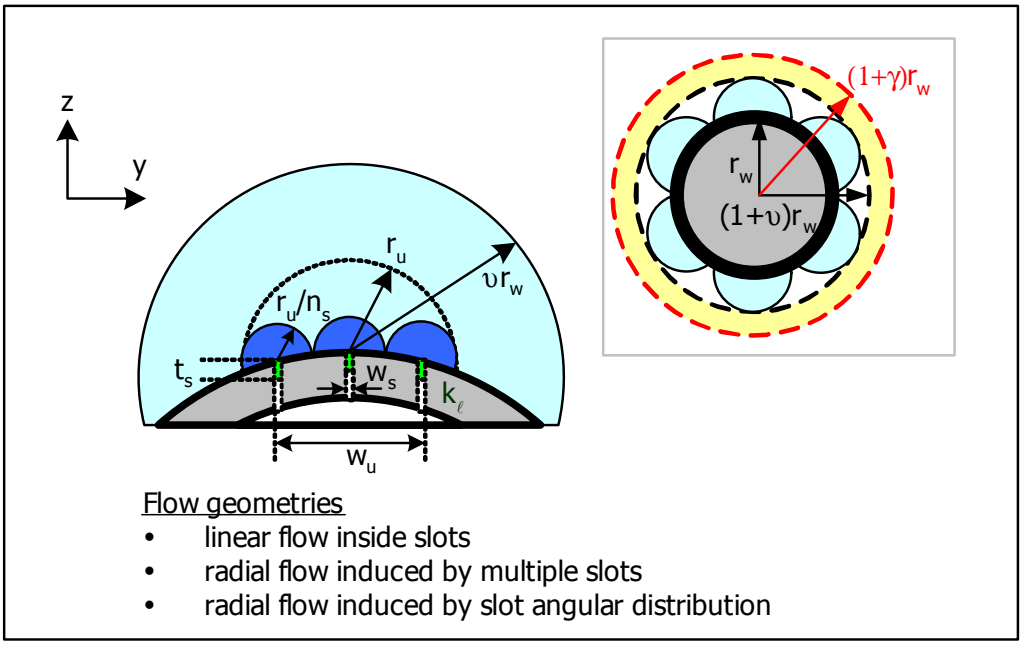

Figure 2.10 Flow geometries around a slotted liner[13]

It was presented in Furui's work that four types of flow regimes exist around a slotted liner (Fig. 2.10). Each flow regime introduces a skin factor which can be calculated by the equations formulated on the basis of finite element simulations performed by the authors.

First flow regime is liner flow inside the slots, which is caused by the plugging of slots by the formation particles. In our case it is assumed that the permeability of slots is much higher than the formation permeability so the skin factor caused by this flow regime is assumed to be zero. Second flow regime is radial flow induced by multiple slots and the skin factor caused by this flow regime, s_1, is given by Eq. 2.42. The inner and outer radii of the radial flow geometry of this regime are denoted by r_1 ($=w_s/4$) and r_2 ($=w_u/2n_s$) respectively.

$$s_1 = \left(\frac{2}{n_s m_s \lambda}\right) \ln\left(\frac{1-\lambda+2l_{Ds}/w_{Ds}}{1-\lambda+n_s l_{Ds}/w_{Du}}\right) \tag{2.42}$$

As it was assumed that the wormholes are considered as infinite conductivity channels (no pressure drop occurs in the wormholes) so it can be assumed that when the wormholes cross this regime (i.e. when $r_{wh}>r_2$) the skin factor caused by this flow regime s_1 reduces to zero.

The third flow regime is radial flow induced by the angular distribution of slot units which exists in the region from r_2 ($=w_u/2n_s$) to r_3 ($=\upsilon r_w$). The skin factor caused by this flow regime is defined by Eqs. 2.43 and 2.44 as,

For high slot penetration ratio ($\gamma<\upsilon$),

$$s_2 = \left(\frac{2}{m_s}\right)\left[\frac{1}{\lambda}\ln\left(1-\lambda+l_{Ds}/w_{Du}\right)+\ln\left(\frac{2\lambda\upsilon}{l_{Ds}}\right)\right] \tag{2.43}$$

And for low slot penetration ratio ($\gamma>\upsilon$),

$$s_2 = \left(\frac{2}{m_s\lambda}\right)\ln\left(\frac{1-\lambda+l_{Ds}/w_{Du}}{1-\lambda+l_{Ds}/2\upsilon}\right) \tag{2.44}$$

where υ and γ are defined by Eqs. 2.45 and 2.46 respectively.

$$\begin{cases} \upsilon = Sin(\pi/m_s) & ms \neq 1 \\ \upsilon \approx 1.5 & ms \neq 1 \end{cases} \tag{2.45}$$

$$\gamma = \frac{l_{Ds}}{2\lambda} \tag{2.46}$$

As the wormhole crosses radius r_3 this radial skin component reduces to zero (i.e. $s_2=0$ for $r_{wh}> r_3$).

The fourth flow regimes exists due to radial flow away from the liner and it stretches from radius r_3 ($=\upsilon r_w$) to r_4 ($=r_b$). r_b is the distance to a point far away from the center of the wellbore which has no importance as it ultimately cancels out. The skin factor caused by this flow regime can be written as s_3 and it can be defined by Eqs. 2.47 and 2.48.

For high slot penetration ratio ($\gamma<\upsilon$),

$$s_3 = \ln\left(\frac{r_{Db}}{1+\upsilon}\right) \tag{2.47}$$

And for low slot penetration ratio ($\gamma>\upsilon$),

$$s_3 = \left(\frac{l_{Ds}/\lambda}{l_{Ds}-2(1-\lambda)}\right)\ln\left\{\left(\frac{\lambda+l_{Ds}/2}{1+\upsilon}\right)\times\left[1+\frac{2\upsilon(1-\lambda)}{l_{Ds}}\right]\right\}+\ln\left(\frac{r_{Db}}{1+\frac{l_{Ds}}{2\lambda}}\right) \tag{2.48}$$

In the ideal conditions when there is no fluid path diversion, i.e. all the fluid particles are following the radial flow pattern from r_b to r_w. The skin factor s_4 can be defined by Eq. 2.49 as;

$$s_4 = \ln(r_{Db}) \tag{2.49}$$

The skin for the radial flow geometry, $s_{SL,r}$, can be calculated by adding s_1, s_2 and s_3 and by subtracting s_4. As the wormhole passes crosses each flow regime the particular skin factor caused by that flow regime is to be reduced to zero.

When formation damage is present around the wellbore completed with slotted liner the skin effect is magnified. The change in this skin factor during the wormhole propagation can be determined using the equations presented in previous section for horizontal wells with Openhole completions. The complete equations for a slotted liner in presence of formation damage around the wellbore is given as,

$$s = \left(k/k_d - 1\right)\ln\left(r_d/r_w\right) + s_{SL,r}k_d/k \tag{2.50}$$

2.5.4 Partial penetration skin model

Acid injection in long horizontal wells is often into relatively short, isolated sections of the well. Because the section treated is connected to the entire reservoir, the injectivity is higher than it would be if the reservoir ended at the end of the completion interval. A partial penetration skin factor can be used to account for this effect. This partial penetration effect is important when injecting into relatively small intervals of horizontal wells and is not widely recognized, so a brief review is in order. The effect on productivity of completing a vertical well in only a portion of the reservoir has been described numerous times, beginning with Muskat[15].

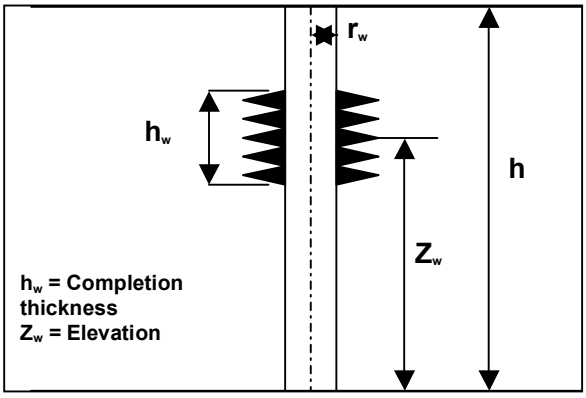

Figure 2.11 A section of partially completed vertical wellbore

For a vertical well completed along a thickness, h_w, in a reservoir of thickness h (Fig. 2.11), and in the absence of any other skin effects, the steady-state productivity index is defined as in Eq. 2.51;

$$J = \frac{kh}{141.2B\mu\left(\ln\frac{r_e}{r_w} + s_c\right)} \tag{2.51}$$

Where s_c is the partial completion skin factor. When h_w is less than h, s_c is positive, accounting for the lessened productivity of the partially completed well. Models to calculate s_c have been presented in many studies, including those of Cinco-Ley et al.[16],

Odeh[17], and Papatzacos[18]. The productivity index could also be written using the completed thickness in the inflow equation;

$$J = \frac{kh_w}{141.2B\mu\left(\ln\frac{r_e}{r_w} + s_c'\right)} \tag{2.52}$$

If h_w is less than h, s_c' must necessarily be negative to give the same productivity index as Eq. 2.51. When h_w is relatively small compared with h, these partial completion effects are large. For example, when hw/h is 0.25, s_c is 8.8 using the Papatzacos model when the completion is centered in an isotropic reservoir. If $\ln(re/r_w)$ is 8, a typical value, the corresponding s_c' is -3.8. Thus, when calculating productivity or injectivity based on the completion zone thickness, the well appears to be stimulated because the reservoir is thicker than the completed interval.

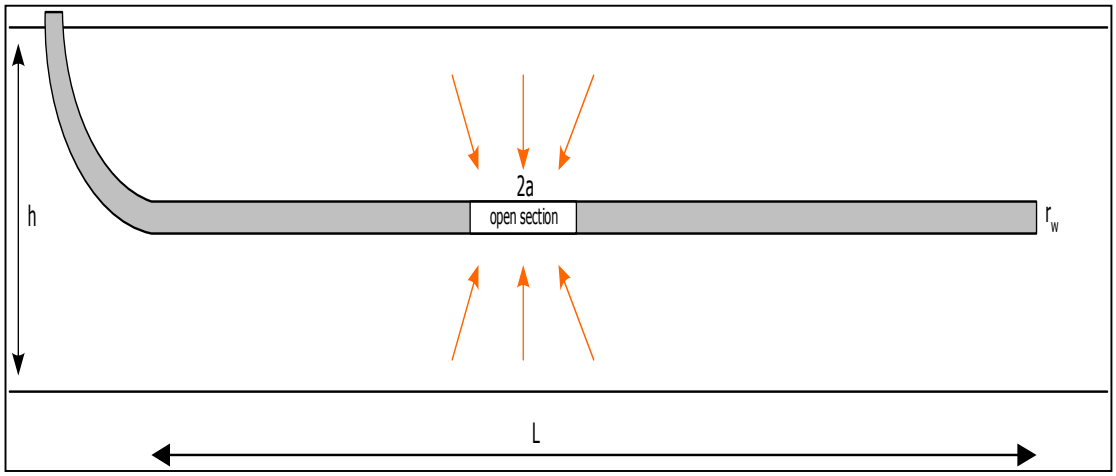

Figure 2.12 Horizontal well partially open to the reservoir

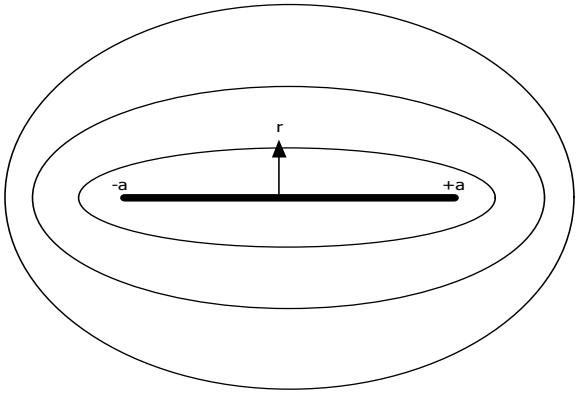

Figure 2.13 Ellipsoidal flow geometry

The corresponding situation for acid injection into a short interval of a horizontal well is shown in Fig. 2.12. Because we are assuming radial flow from the completed interval in our reservoir flow model, there will be a large partial penetration effect which we can account for with a negative skin factor.

A simple model is developed to calculate this type of skin factor as follows. Consider a horizontal well partially open to the reservoir as in Fig. 2.12. Ellipsoidal flow exists due to partial opening of wellbore in the reservoir as in Fig. 2.13. If the formation is isotropic then in prolate spherodial coordinates the pressure drop can be given by; *

$$\Delta p = \frac{141.2 q \mu}{k(2a)} \ln\left(\frac{e^{\xi}+1}{e^{\xi}-1}\right) \tag{2.53}$$

where

$$\xi = \sinh^{-1}(r_D) \tag{2.54}$$

$$r_D = r/a \tag{2.55}$$

The radial flow equation based on a completed interval of length 2*a* is

$$\Delta p = \frac{141.2 q \mu}{k(2a)} \left[\ln\left(\frac{r}{r_w}\right) + s_{pp}\right] \tag{2.56}$$

*Personal communication for horizontal well partial penetration skin with K.Furui, ConocoPhillips, A.D.Hill, and D.Zhu, Texas A&M U., College Station, TX (2007).

We can calculate the pseudo-skin factor due to ellipsoidal flow to the open section. For a centered well, $r=h/2$ (i.e. $r_D=r/a=h/2a$) in Eq. 2.56. Equating the pressure drops given by Eqs. 2.53 and 2.56 provide the horizontal well partial penetration skin factor as,

$$\ln\left(\frac{e^{\xi}+1}{e^{\xi}-1}\right)=\ln\left(\frac{h}{2r_w}\right)+s_{pp}$$
$$s_{pp}=\ln\left[\frac{2r_w(e^{\xi}+1)}{h(e^{\xi}-1)}\right]=\ln\left[\frac{2r_w(r_D+1+\sqrt{r_D^2+1})}{h(r_D-1+\sqrt{r_D^2+1})}\right] \quad (2.57)$$

The partial penetration skin is calculated using Eq. 2.57 and it will be accounted in the total skin factor. This partial penetration skin factor is added to the skin factor calculated from formation damage skin and completion skin models. The overall skin factor is used in the reservoir flow model equation to obtain the solution. It is noted that the partial penetration skin factor remains constant during the matrix acidization process.

2.5.5 Solution of matrix acidizing model

To solve the problem of matrix acidization in a horizontal well, all presented models are integrated and solved in a discretized manner in time and space. Initial and boundary conditions to solve this system of equations are defined as;

$$q_w(x,0)=0$$
$$p_w(x,0)=p_R \quad (2.57)$$
$$q_w(x,t)=0; x\geq L$$

The first and second condition explain that the initial wellbore flow rate at any point is zero (i.e. $q_w=0$) as the wellbore pressure is equal to the reservoir pressure (i.e. $p_w=p_{R)}$. The third condition explains that there is no lateral flow in the wellbore beyond the toe of the well (i.e. $x>L$). Along with these initial and boundary conditions the injection rate at the heel of the well (i.e. $x=0$) is defined as in Equation 2.58;

$$q_w(0,t)=q_i(t) \quad (2.58)$$

In summary, the steps to solve the model equations are as follows:

1. Divide the horizontal wellbore into small segments.
2. Divide the injection time into small time steps.
3. Apply the initial and boundary conditions.
4. Use the skin model to get the skin factors for each segment (Section 2.5).
5. Solve the pressure drop equation (Eq. 2.5) and the reservoir flow equation (Eq. 2.9) to get p_w, q_w, and q_r.
6. Use the interface tracking model (Eq. 2.14) to get the interface locations (x_{int}).
7. Calculate the volume of acid injected into each segment during the time step from the flow distribution and interface locations.
8. Use the wormhole model to get the length of wormholes in each segment at the end of the time step (Section 2.4).
9. Go back to step 4 and loop through the skin factor calculation using new wormhole length.

CHAPTER III

MATRIX ACIDIZING SIMULATOR

3.1 Matrix acidizing simulator

The models for wellbore flow, partial penetration and completion skin factor, front tracking, reservoir inflow, wormhole growth, and skin evolution are incorporated together to obtain the solution of acidizing in a horizontal well. To achieve this wellbore is divided into small segments and equations for wellbore material balance, wellbore pressure drop and reservoir inflow needs to be written in discretized form. As stated in Chapter II initial and boundary conditions are applied to solve the equations.

A simulator is developed implementing all the models and solution scheme described in APPENDIX A. The simulator implements the theoretical models developed in this study. The models determine the volume of acid injected (bbl/ft) as a function of position along the wellbore by tracking the movement of the acid in the wellbore and the formation. For matrix acidizing treatments, the model also predicts the depth of penetration of wormholes as a function of position along the zone. Skin factor is calculated after wormhole length is obtained from the wormhole models. Pressure, injection rate, wormhole length and skin factor distribution along the injection intervals of the well will be the final output of the simulator.

The acid placement simulator model equations are developed in FORTRAN-90. The simulator reads the data from the input data file. This input data file contains the information about the well completion and reservoir properties along the length of wellbore. A sample input data file is shown in APPENDIX B.

The simulator also provides bottomhole pressure at the heel as output for a defined injection rate schedule. This simulated pressure can be used as a tool to analyze the past treatments for which the observed bottomhole pressure data are available.

3.2 Simulator data files

The input data file contains the information about the well completion and reservoir properties along the length of wellbore. The output data files contain the calculated values of the various parameters. A list of various files used by the simulator is given in Table 3.1.

Table 3.1 Matrix acidizing simulator data files

DATA FILE	TYPE	FILE INFORMATION
data.acm	Input file	Contains well completion, reservoir data, and acid treatment data
pwheel.acm	Output file	Pressure history at the heel of the well
qwheel.acm	Output file	Injection rate history at the heel of the well
pgauge.acm	Output file	Pressure history at the surface gauge
stot.acm	Output file	Total skin factor history
pindex.acm	Output file	Productivity index history
pw.acm	Output file	Injection pressure in each grid block at the end of each stage
qsr.acm	Output file	Specific injection rate in each grid block at the end of each stage
vinj.acm	Output file	Injected acid volume in each grid block at the end of each stage
skin.acm	Output file	Skin factor in each grid block at the end of each stage
lwh.acm	Output file	Wormhole length in each grid block at the end of each stage
pvbt.acm	Output file	Pore volume for break through in each grid block at the end of each stage

3.2.1 Input data file

The input file (data.acm) contains the information about the well completion, reservoir properties and acid treatment. A sample input data file for the simulator is presented in APPENDIX B. The comments lines starts with dash and are provided as a help to facilitate the input data entry. It contains four sections separated by different keywords.

The first section starts with the keyword %WRC and it contains information of well completion and reservoir properties. The casing and tubing diameter are defined in this section. The number of grid cells required in a horizontal well is also defined in this section and property of each grid block such as grid block length, porosity, permeability, perforation details, initial damage; initial damage radius etc can be defined individually.

The next section starts with the keyword %INJ and it contains the injection treatment information. The boundary condition needed for the solution is defined as constant rate or constant pressure. The injection rate schedule is to be defined in case of constant rate boundary condition to get the simulated pressure at the heel as output. The pressure values at different time step can be supplied as input to the simulator in case of constant pressure boundary condition. The next section starts with the keyword %IFP and the injected fluid information is given as input. This section provides a tool to handle the injection of multiple fluids such as water, acid etc. The selection of wormhole model is facilitated with the help of next section which starts with the keyword %WHM. The volumetric wormhole model needs the pore volume for breakthrough (PV_{bt}) as input. For Buijse's semiempirical model two inputs are needed which are optimum pore volume for breakthrough ($PV_{bt\text{-}opt}$) and optimum injected fluid velocity ($V_{i\text{-}opt}$). Irrespective of the selected wormhole model these input parameters are determined from the core flow experiments performed in the lab. The input data file end with the keyword %END which tells the simulator that it has reached the end of the file and the input data reading process terminates.

3.2.2 Output data files

Table 3.1 provides a detailed list of various output data files of the simulator. The output of acid placement simulator includes the skin, wormhole length, acid coverage along the length of the wellbore at changing time steps. It provides the variation of bottomhole pressure, injection rate, and productivity index with time. The location of fronts created between several injected fluids is also included in output. The output files generated from the FORTRAN program can be opened with the notepad. The output data from these files can be edited in MS Excel for output data processing.

CHAPTER IV

RESULTS

A set of simulations were performed using the acidizing simulator for long horizontal wells. These results provide a better understanding of how acid is distributed in a wellbore. It is also analyzed that how well and reservoir parameters affect the results. The output of the hypothetical cases and study of an actual treatment are presented in this chapter.

4.1 Hypothetical examples

In these examples, the effects of acid volume and acid injection rate on the placement of injected acid and the resulting distribution of acid along the well are investigated. The completion of horizontal well affects the acidizing performance. Matrix acidizing in openhole completions, cased-perforated completions, and slotted liner completions are discussed separately in different subsections.

4.1.1 Horizontal well with openhole completion

In this example, acid is injected at a relatively low rate into a long section of a horizontal well. This is the situation where wellbore flow conditions are most likely to be significant. The conditions for this case are presented in Table 4.1. A uniform distribution of permeability, porosity, initial damage ratio, and initial damage radius along the length of the wellbore is assumed. The volumetric model of wormhole growth was used in the acidizing simulator to model the wormhole growth.

Assuming that the acid is being injected from a tubing tail located at one end of the completed interval, the progression of acid placement with time is shown in Fig. 4.1. By the end of 200 barrels of acid injection at 100 minutes of pumping time, acid has not yet reached the far end of the completed interval. For better acid coverage with this small volume treatment (the total volume pumped in 100 minutes is only 8.4 gal/ft), some method of diversion is required.

Table 4.1 Data for acid injection into horizontal well with openhole completion

Well length	1000 ft
Number of grid blocks	50
Grid block length	20 ft
Completion	Open hole
Damage radius	0.5 ft
Permeability	2 md
Index of anisotropy	1
Permeability impairment ratio	0.5
Reservoir rock	Limestone
Acid	15 % Hcl
Reservoir pressure	3200 Psi
Wormhole model	Volumetric
Pore volume for breakthrough (PV_{bt})	2
Injection rate	2 bpm
Duration of pumping	100 Min

The distribution of wormhole lengths along the wellbore created by this acid injection is shown in Fig. 4.2. By 100 minutes of acid injection, wormholes had extended 6 inches into the formation at the heel of the completed interval. Injection of larger volumes of acid improves the coverage of acid in this long interval. With 500 bbl of acid injected, the far end of the completed interval has received a significant amount of acid injection, with good acid coverage along most of the interval (Fig. 4.3). For a well with only minor damage, as was assumed for this case, although the acid is increasing the local injectivity, and thus retarding the progress of the acid down the wellbore, the injectivity is changing slowly, and thus does not have a strong effect on the acid placement. Another illustration of this is obtained by changing the efficiency of the acid treatment by changing the PV_{bt} parameter used in the volumetric model. Fig. 4.4 compares the acid placement for cases ranging from PV_{bt} of 0.5 (very rapidly propagating wormholes) to inert fluid (no wormholes, hence no change in injectivity during injection). The acid

coverage changes a little depending on how efficiently the acid is increasing injectivity of the formation, but it is not a large effect. One of the interesting predictions of this model is the downhole pressure response during acid injection. Bottomhole pressure measurements are becoming more and more common during acid injection and can provide very useful diagnostic information about the treatment. The predicted pressure responses for a wide range of PV_{bt} are shown in Fig. 4.5. When an inert fluid is injected, the pressure builds up because of the transient nature of the reservoir flow. With acid injection, the simultaneous stimulation is tending to decrease the injection pressure. Thus, depending on how efficiently the acid is increasing the near-well permeability, the injection pressure may rise or fall, as shown in Fig. 4.5. Comparison of actual treatment response with predictions like these provide a means of diagnosing the effectiveness of acid stimulation and if done in real time can be used to optimize a treatment on the fly.

The final aspect of this hypothetical case is the effect of the wormhole model on the predicted acid placement. With the Buijse model, the wormhole propagation is varying with acid flux, with the maximum wormhole propagation being at the optimal injection condition. In this particular case, the acid fluxes are near the optimum, but somewhat higher. For the range of acid fluxes occurring in this treatment, the PV_{bt} from the Buijse model varies from about 2 to about 2.5 (Fig.4.6). Fig. 4.7 shows the wormhole length distribution from the volumetric model with PV_{bt} set to 2.5 compared with the predicted placement using the Buijse model with the $PV_{bt\text{-}opt}$ equal to 1.5. The volumetric model, which assumes a constant PV_{bt} independent of acid flux, gives a similar prediction of acid placement, and hence, wormhole distribution, when a value of 2.5 was used for PV_{bt}.

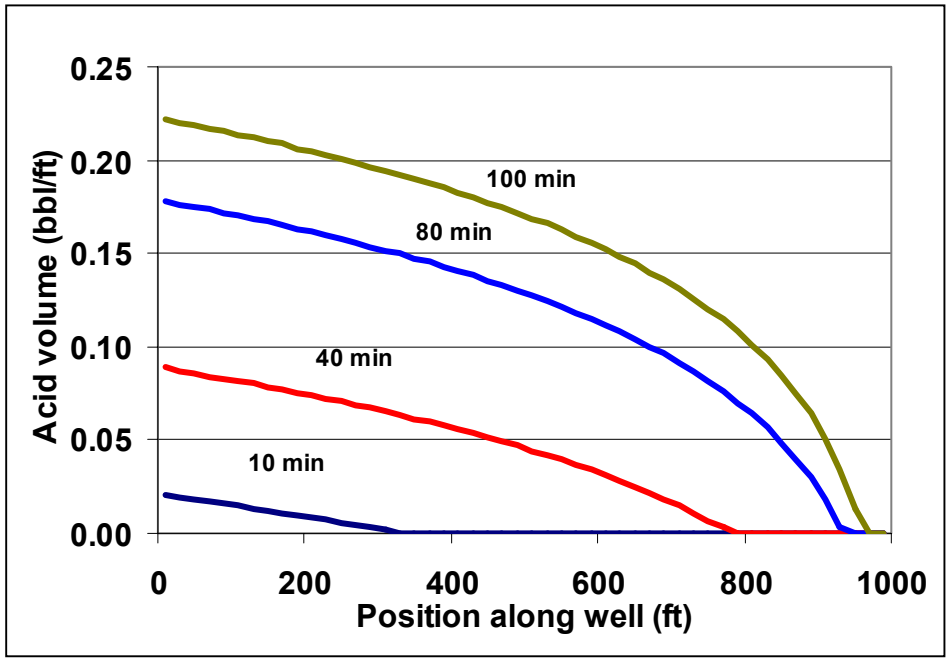

Figure 4.1 Acid coverage over the entire length of wellbore

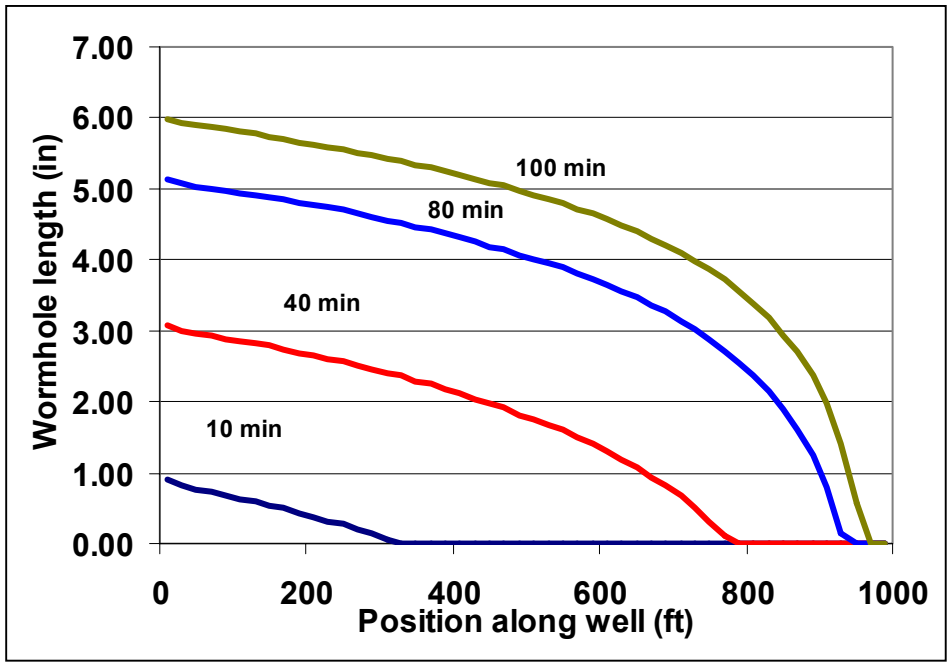

Figure 4.2 Wormhole length distributions at different times

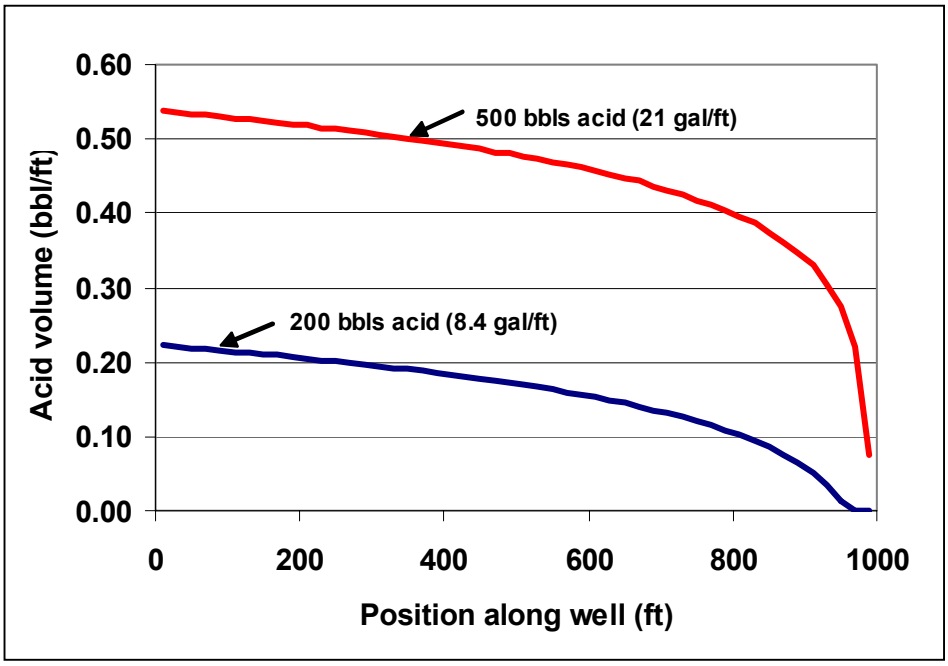

Figure 4.3 Acid placement profiles for 200 and 500 bbls of acid

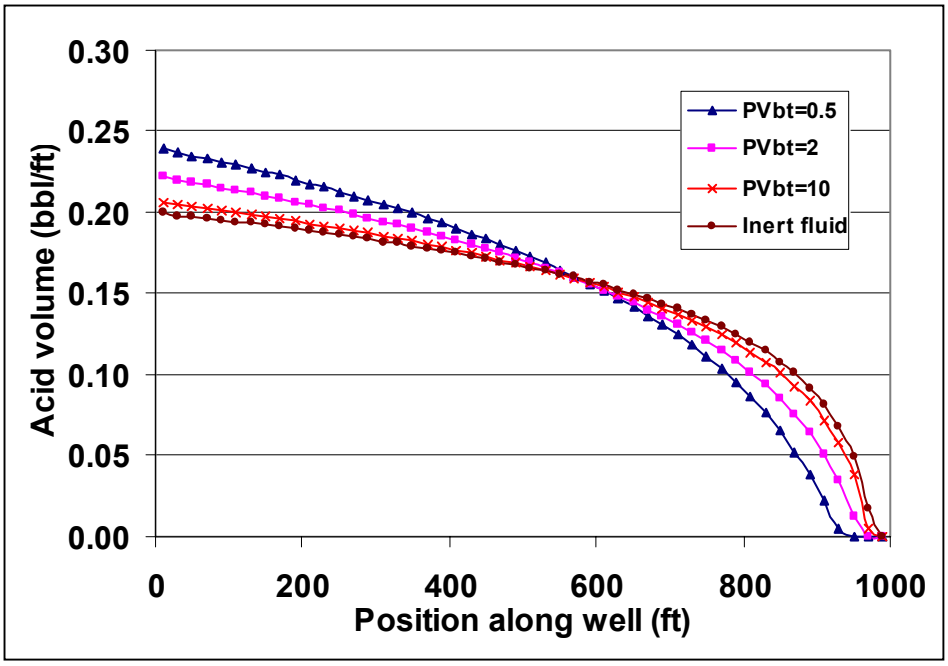

Figure 4.4 Acid placement profiles for different values of PV_{bt}

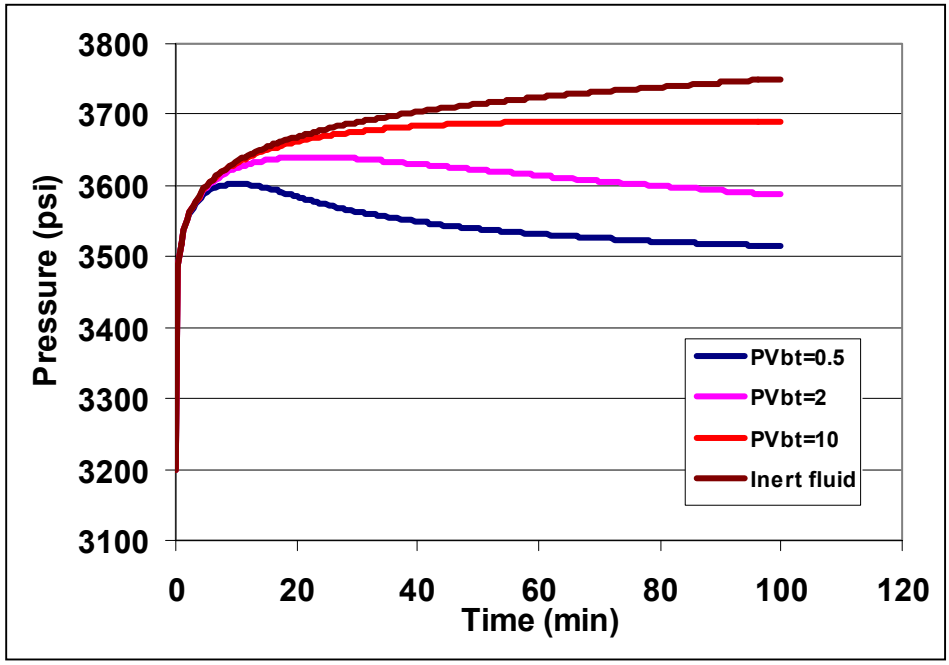

Figure 4.5 Pressure responses during acid injection

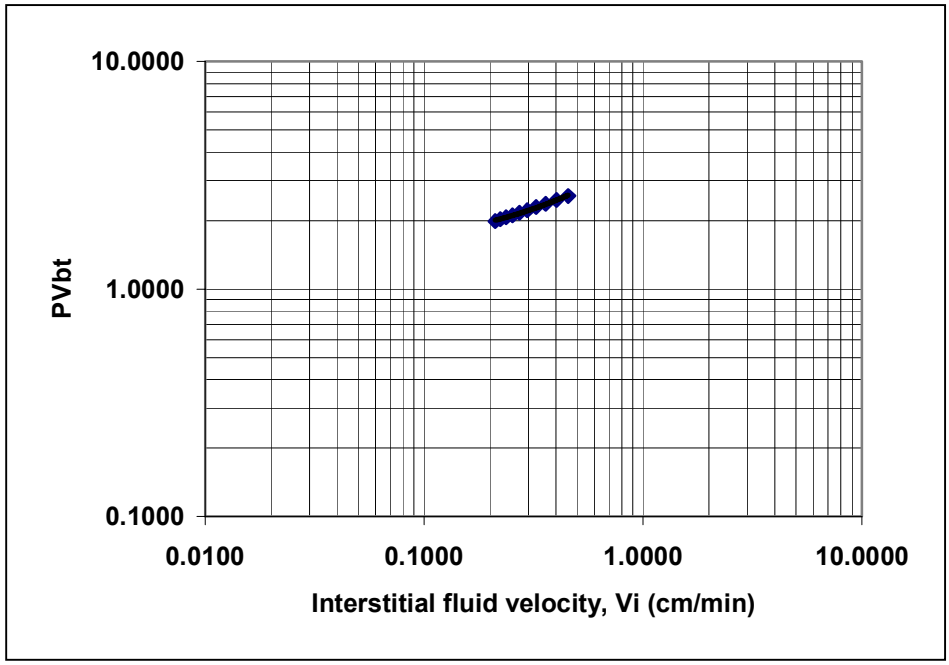

Figure 4.6 PV_{bt} versus V_i during simulation using Buijse Model with $PV_{bt\text{-}opt}$=1.5

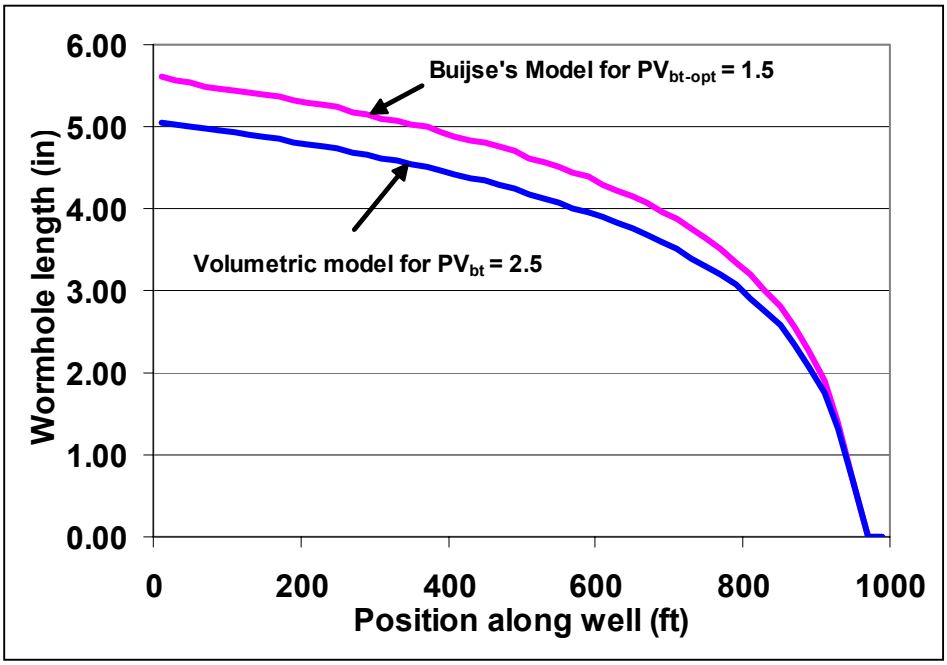

Figure 4.7 Comparison of wormhole distributions from the volumetric and Buijse's models

4.1.2 Horizontal well with cased-perforated completion

It is described in the Chapter II that skin factor evolution in cased-perforated completions is different from the openhole completions. The increase in the length of wormhole is added to the perforation length at the end of time step to calculate the new perforation length. This new perforation length is provided to the skin model to calculate the new skin factor at the end of time step. The data used in simulating the results for this case is presented in Table 4.2.

In this example, the perforation length varies from 9 to 13 inches from heel to toe of the well. The distribution of perforation length along the length of wellbore is shown in Fig. 4.8. This variation in length is adopted as Gdanski referred in his work that by having higher injectivity at the toe helps in achieving a uniform coverage of the acid. The part of wellbore lying towards the toe receives less acid when compared to the part of the wellbore lying towards the heel. By putting longer perforations towards the toe of the well would certainly results in a better stimulation.

Table 4.2 Data for acid injection into horizontal well with cased-perforated completion

Well length	1000	ft
No. of grid blocks	50	
Grid block length	20	ft
Completion	Cased perforated	
Damage radius	1	ft
Permeability impairment	0.5	
Permeability	2	md
Index of Anisotropy	1	
reservoir rock	Limestone	
Acid	15% Hcl	
reservoir pressure	3200	Psi
wormhole model	Volumetric	
PV_{bt}	3	
injection rate	2	bpm
duration	100	min
Perforation data		
m_p	2	
Perforation length (l_p)	9-13	inches
d_p=	0.3	inches
N_p=	1	spf
α=	90	degree
$Rk_{cz}=k_{cz}/k$=	1	
d_{cz}=	0.0003	inches

The simulations results for the above data are shown in Figs. 4.9 - 4.12. In Fig. 4.9, the evolution of skin is shown at different time steps of 10 min, 40 min, 80 min, and 100 min. The skin is less in those areas which have long perforation lengths (i.e. towards the toe). In Fig. 4.10 the acid coverage along the length of the wellbore is shown and it is increasing towards the toe. The acid coverage supports the claim that putting longer perforations towards the toe of the well improves acid coverage. The part of the wellbore towards the toe has received more acid thus an improved stimulation. Fig. 4.11 presents the distribution of wormholes along the length of the wellbore. It is evident from this figure that the wormhole distribution imitates the acid coverage pattern. Fig. 4.12 shows a comparison between two cases i.e. acid injection into a horizontal lateral with uniform

and non-uniform distribution of perforation length. It can be concluded that by putting the longer perforation at the toe of the well certainly would place the acid in the parts of the wellbore which need stimulation e.g. the area towards the toe of the wellbore.

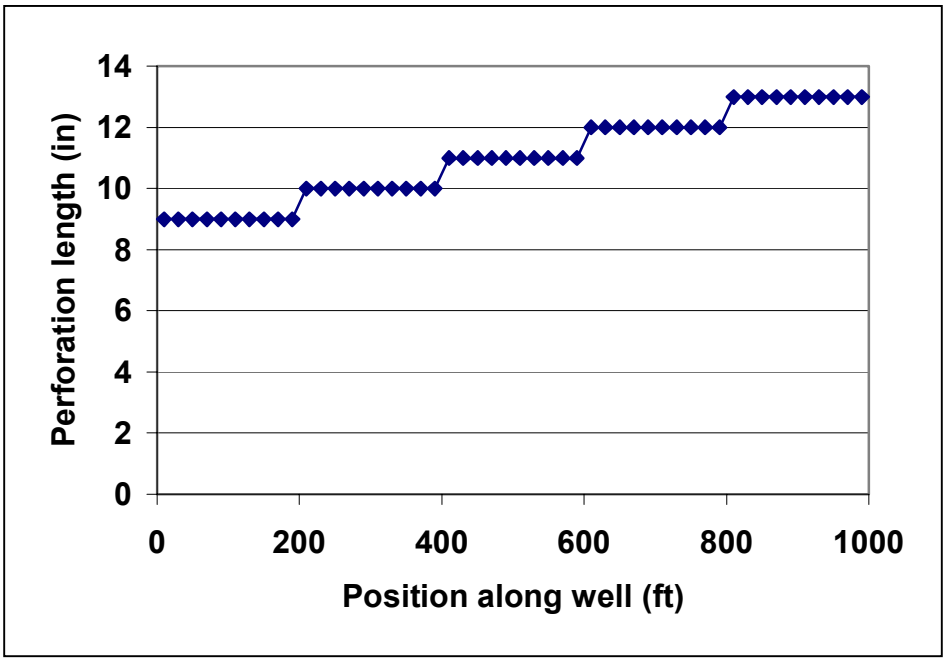

Figure 4.8 Distribution of perforation length along the wellbore

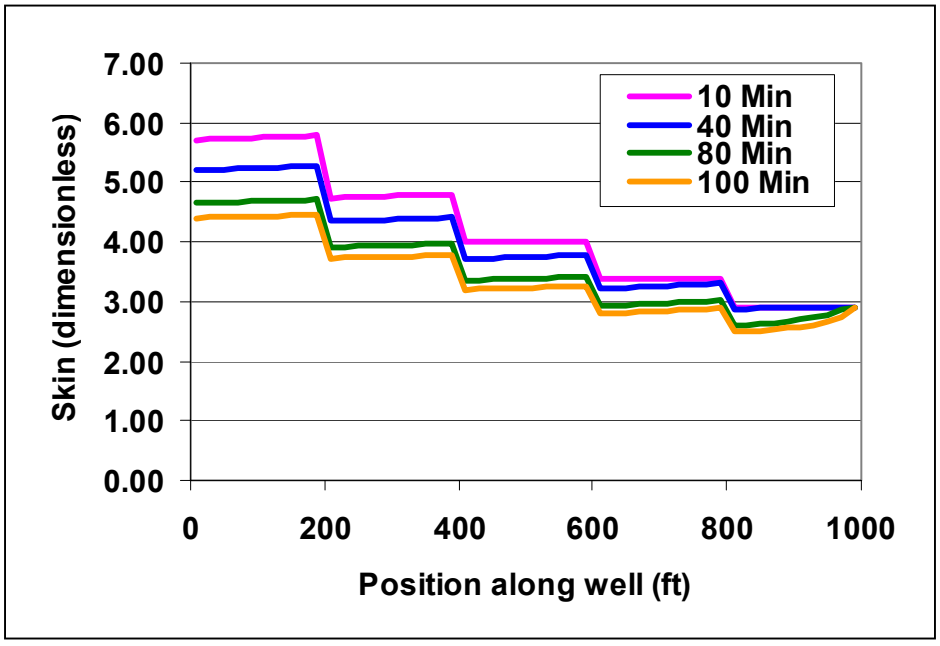

Figure 4.9 Evolution of skin with time during acid injection

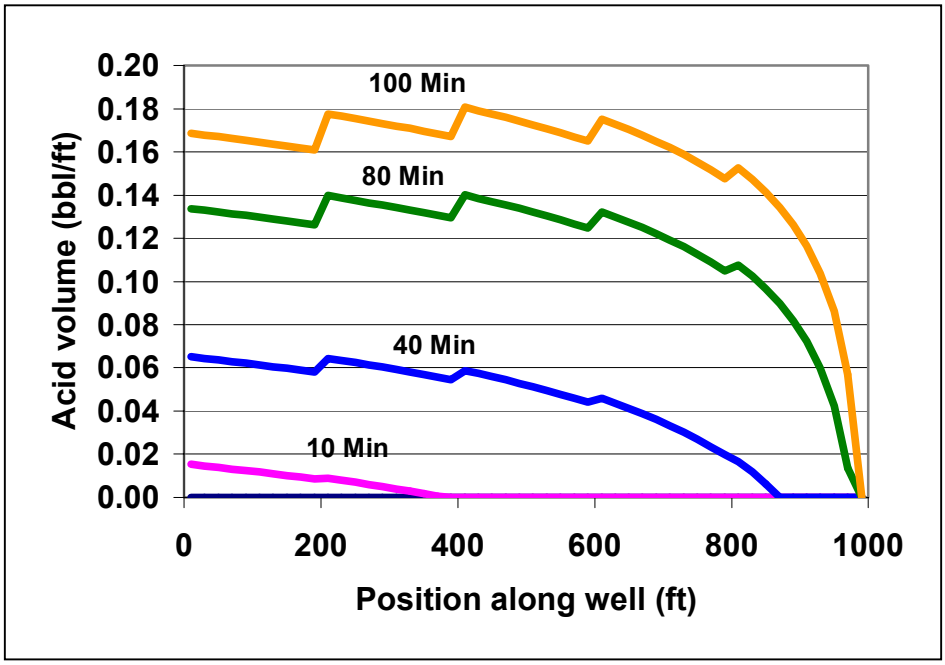

Figure 4.10 Acid coverage in cased-perforated completion case

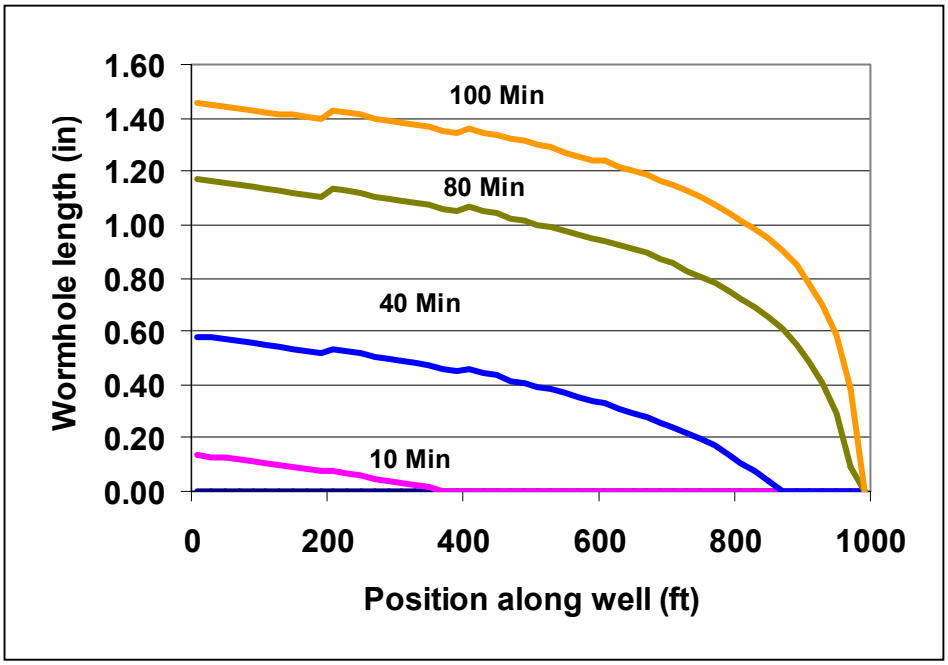

Figure 4.11 Distribution of wormholes in cased-perforated completion case

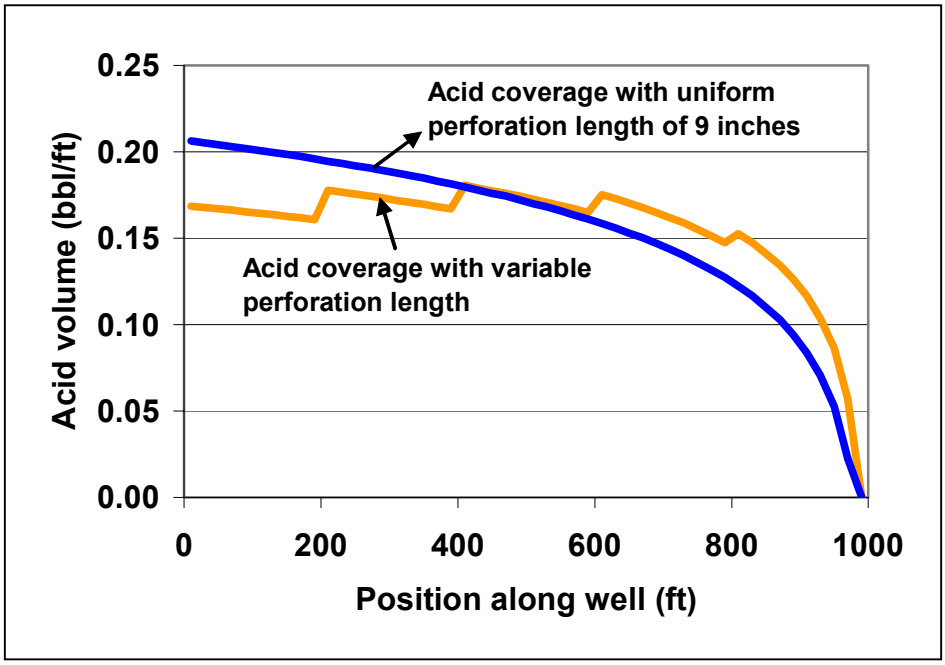

Figure 4.12 Comparison of acid coverage in uniform and non-uniform perforation length distribution

4.1.3 Horizontal well with slotted liner completion

The horizontal well can be completed with slotted liners in unconsolidated formations. It is described in Chapter II that various flow regimes exists around the slotted liner. Each flow regimes causes an additional pressure drop which can be quantified as skin factor. In carbonate formations wormhole crosses through each flow regime reducing the skin factor caused by each flow regime. The statement is true as wormholes are considered as infinite conductivity channels. A simulation was made using the data presented in Table 4.3.

Figures 4.13 and 4.14 show the wormhole length distribution and skin distribution at different time steps respectively along the wellbore. In presence of formation damage around the slotted liner the overall skin magnifies and it can be seen from the Fig. 4.14 that s=3.2 in the parts of the wellbore which are not stimulated. It was explained in Chapter II that a second flow regime is caused by multiple slots exists from region r_1 to r_2. In this case $r_2=w_w/2n_s$= 0.25 inches. There is a drop in skin factor for when the

wormhole length crosses this region (i.e. $>r_2$). Furthermore there exists a flow regime extending from r_2 to r_3 where $r_3= vr_w$=0.91 inches. It is evident from Fig. 4.14 that the skin factor takes a further drop in all those zones where the wormhole length has crossed the third flow regime (i.e. r_3). The formation of wormhole might overcome the completion skin caused by various flow regimes around a slotted liner. Matrix acidizing can be used as a tool to enhance the productivity from the horizontal wells completed with slotted liners.

Table 4.3 Data for acid injection into a horizontal well with slotted liner completion

Well length	1000	ft
No. of grid blocks	50	
Grid block length	20	ft
Completion	Slotted liner	
Damage radius	0.5	ft
Damage impairment	0.5	
Permeability	2	md
Index of Anisotropy	1	
reservoir rock	Limestone	
Acid	15% Hcl	
reservoir pressure	3200	Psi
wormhole model	Volumetric	
PV_{bt}	3	
injection rate	2	bpm
duration	30	min
Slotted liner data		
m_s	12	
O_s	0.059	
n_s	2	
w_s	0.5	inches
l_s	2	inches

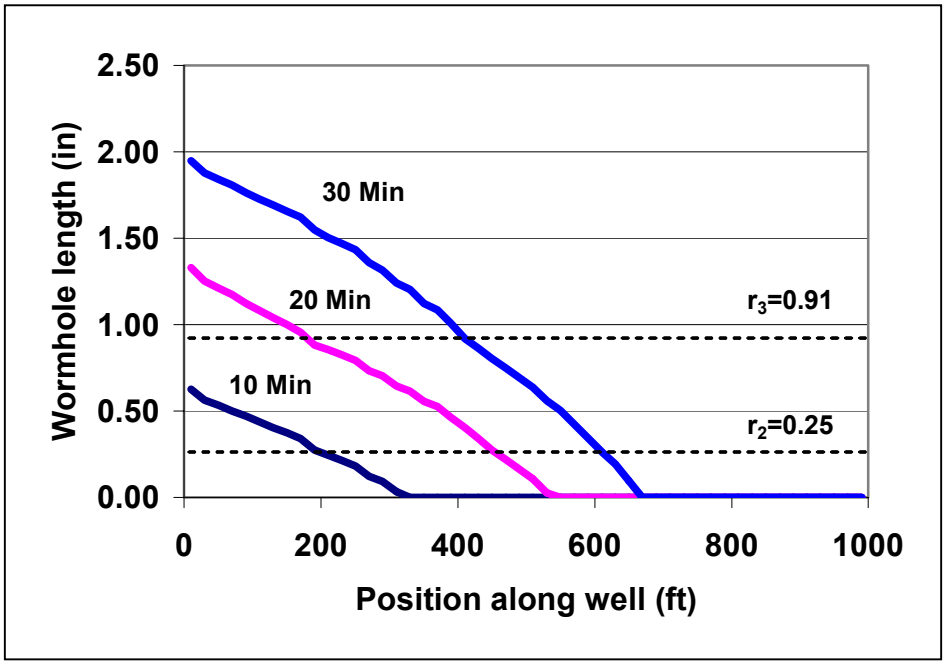

Figure 4.13 Distribution of wormhole length in slotted liner completion

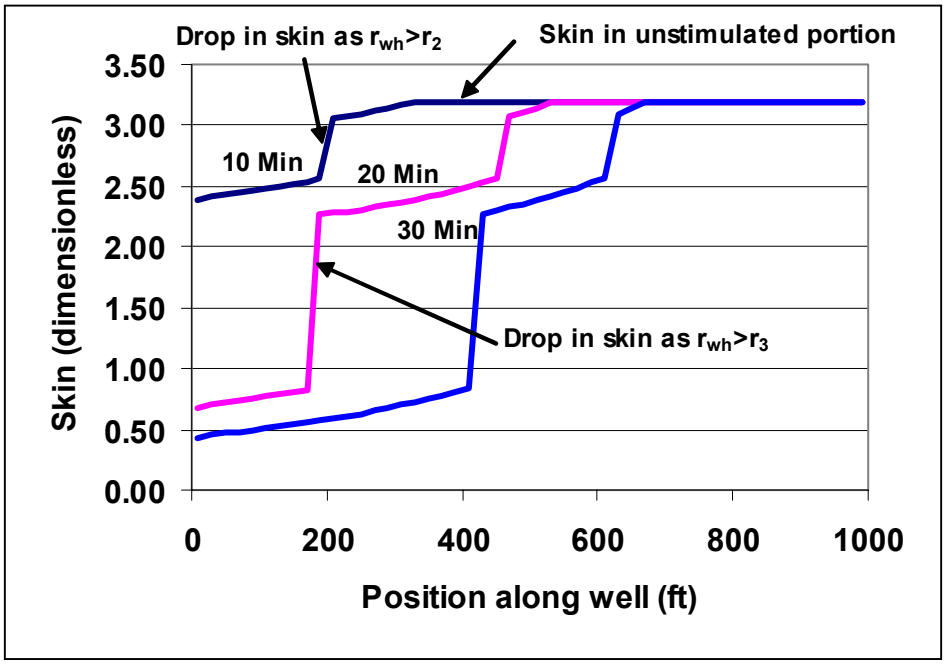

Figure 4.14 Distribution of skin in slotted liner completion

4.1.4 Heterogeneity effect in horizontal well acidizing

When using long horizontal well in carbonate reservoirs with heterogeneous reservoir properties along the length of wellbore, most of these wells often encounter thief zones (zones of high permeability. These zones can consume much of the injected acid during the treatment thus affecting the overall acid distribution. It is planned to study the effect of acid injection into the wells with thief zones. The data used in this case is listed in Table 4.4.

The initial damage and permeability is varying along the length of wellbore and their distribution is shown in Figs. 4.15 and 4.16. Buijse's model is used in simulation and it provides a decrease in wormhole growth rate with respected to increasing wormhole length. The wellbore encounters three thief zones which are located at 1000 ft, 2000 ft, and 3000 ft from the heel of the wellbore.

Table 4.4 Data for acid injection into a horizontal well with thief zones

Well length	4000	ft
No. of grid blocks	200	
Grid block length	20	ft
Completion	Openhole	
Permeability	2-8	md
Permeability impairment ratio	0.5	
Index of Anisotropy	1	
Reservoir rock	Limestone	
Acid	15% Hcl	
Reservoir pressure	3200	Psi
Wormhole model	Buijse	
$PV_{bt\text{-}opt}$	1.5	
$V_{i\text{-}opt}$	0.1	cm/min
Injection rate	20	bpm
Details for thief zones		
Location	1000,2000,3000	ft
Length	20	ft
Permeability	1000	md

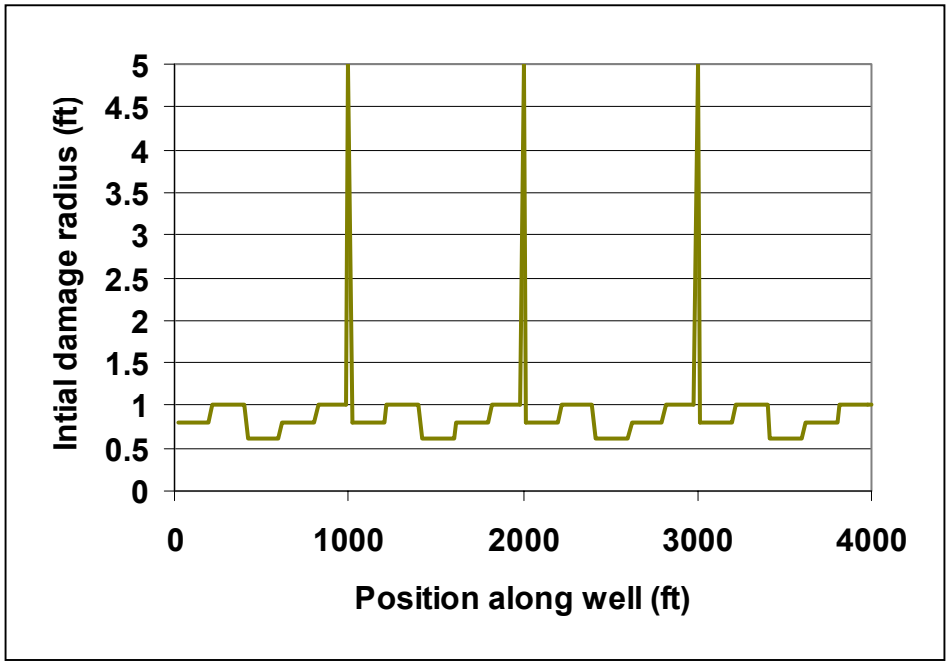

Figure 4.15 Distribution of initial damage along the length of wellbore

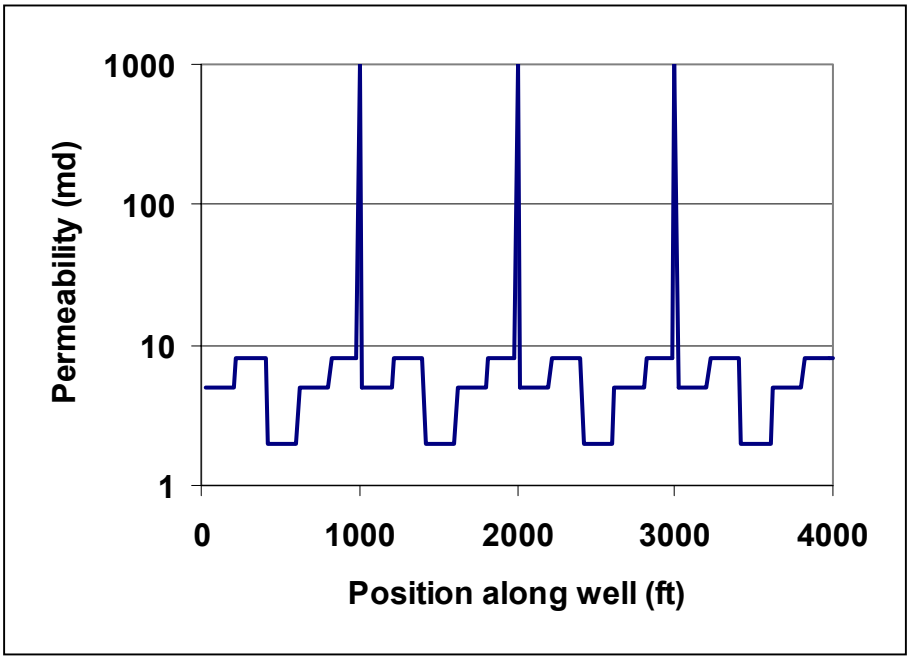

Figure 4.16 Distribution of permeability along the length of wellbore

The acidizing treatment has been continued until the 100 gal/ft (9523 bbl injected acid volume). It has been observed that each thief zone consumed approximately 4500 gal/ft of injected acid, and the rest of the well has received approximately 31 gal/ft of injected acid which is sufficient to propagate the wormholes through the damaged zone. Fig. 4.17 shows a plot of acid coverage along the length of wellbore comparing two situations at different time steps. It shows from Fig. 4.17 that at the end of the injection, most of the wellbore receives uniform acid coverage. The acid coverage volume is high in zones of high permeability, and is low in zones of low permeability. The distribution of wormholes imitates the acid coverage curve. The injectivity index from the start to end of the job is shown in Fig. 4.18 which indicates that after the initial decrease the PI starts increasing sharply and maintains a flat trend after 250 minutes of injection. Fig. 4.19 shows local skin factors at the end of simulation. Even though at the end of the treatment, the most of the wellbore received sufficient acid, without thief zones, the uniform acid distribution can be achieved much faster than the shown case. It is realized that the thief zones that take most of the injected acid should not be treated (due to high permeability), diversion is obviously necessary in such cases.

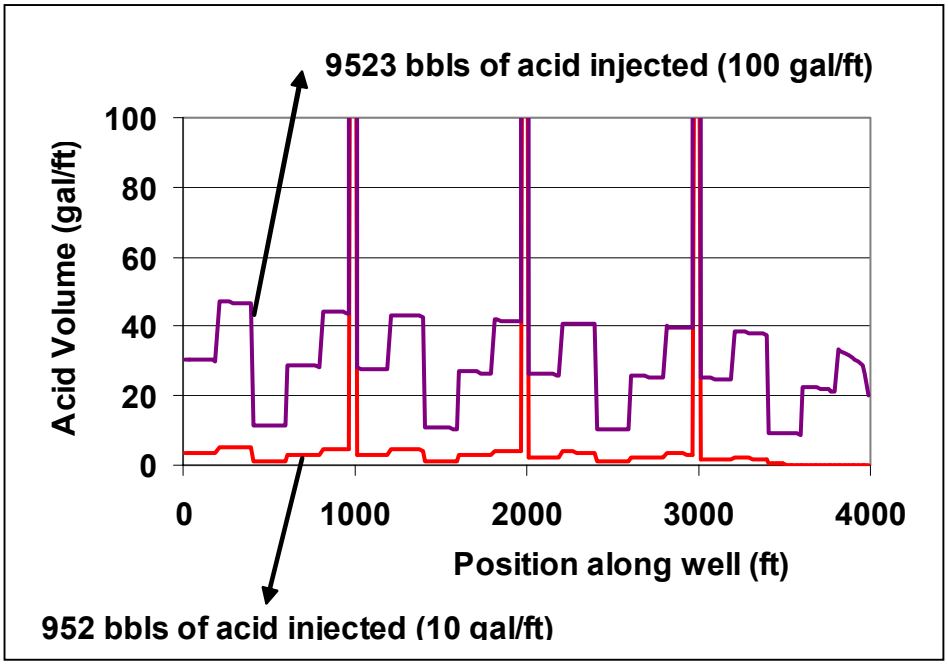

Figure 4.17 Acid coverage along the length of wellbore

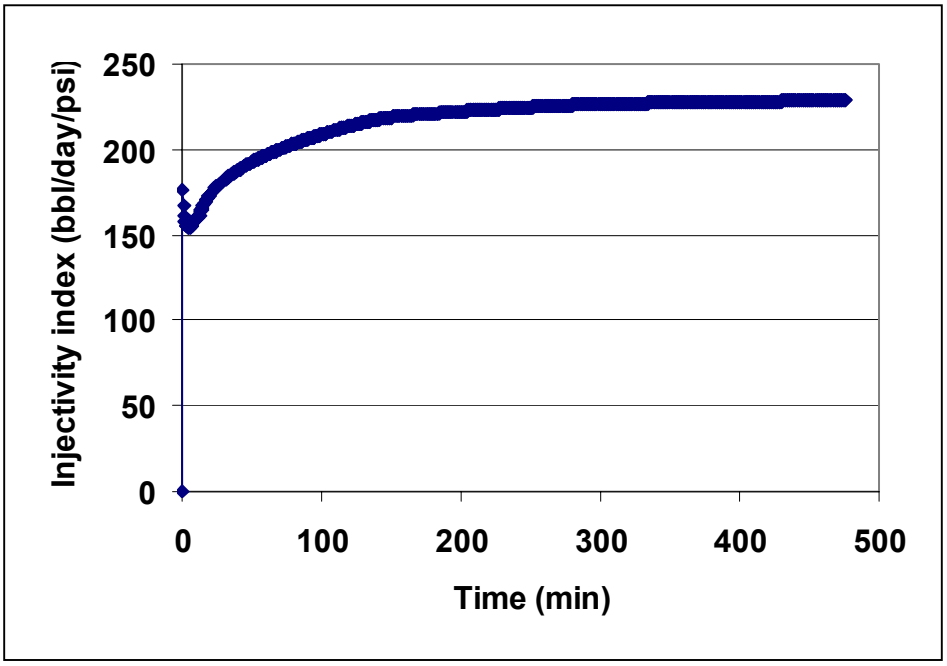

Figure 4.18 Injectivity index during the acid injection

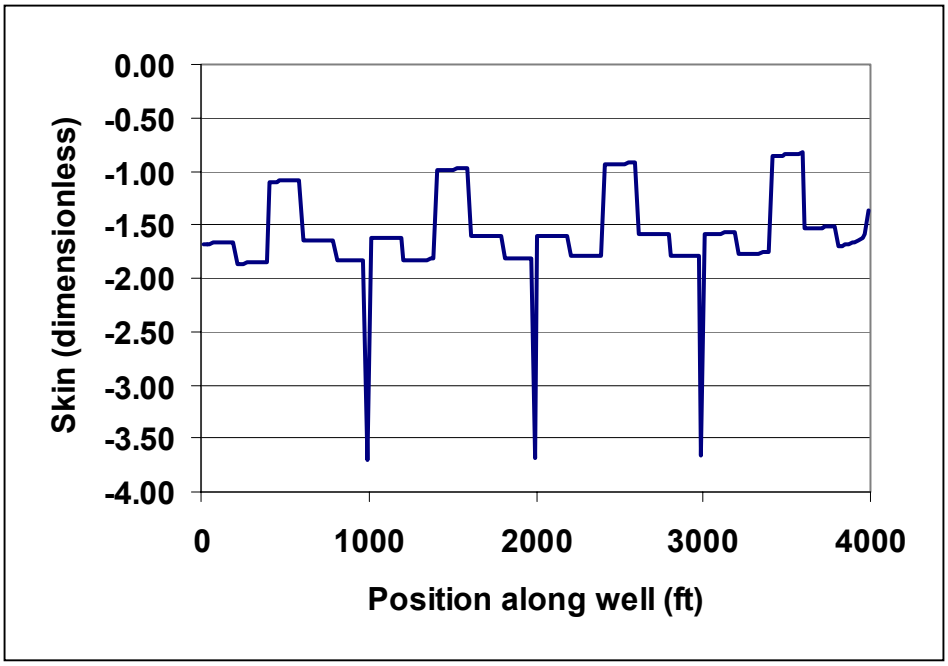

Figure 4.19 Local skin factors along the wellbore at the end of simulation

4.2 Field study

In this field study, predictions for an actual North Sea horizontal well completed in a chalk formation are presented. It is a case where short intervals of the wellbore are treated with the high volume of acid**.** The 6000-ft long horizontal well was completed with sixteen individual 10 foot-long perforated intervals spaced along the well. Each interval is perforated with one shot per foot with the perforations oriented downward. In this stimulation treatment, each zone was isolated with packers (Fig. 4.20) and individually treated with 15% HCl. The treating string was equipped with pressure gauges between the packers and on either side of the packers enabling the operator to monitor the downhole treating pressure and to determine if the packers were set and not leaking. We used our acid placement model to history match the treating pressure response for one of the zones treated.

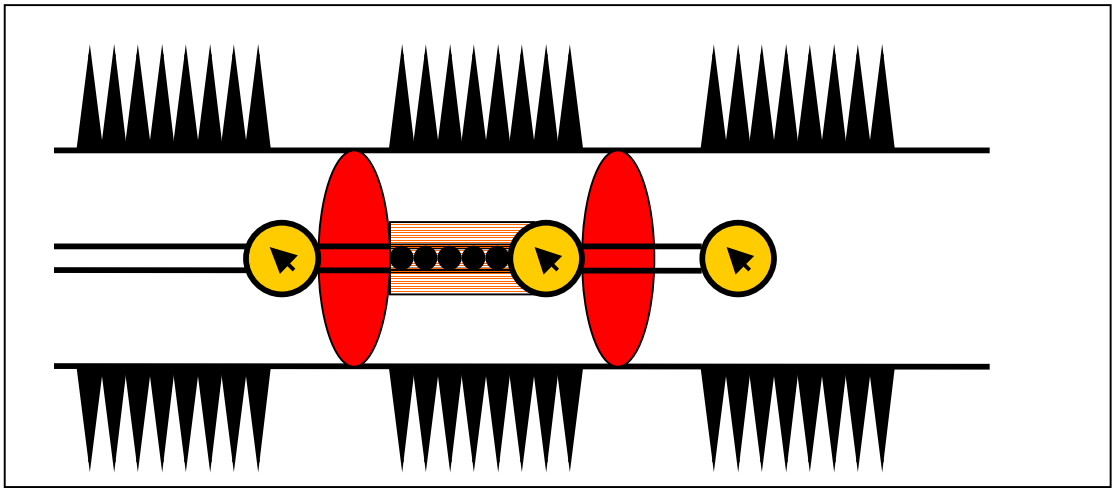

Figure 4.20 Selective stimulation for each perforated zone using straddle packers and perforated coiled tubing

The pressure records from the three downhole gauges are shown in Fig. 4.21. There is a clear indication of the packers being set. The pressure gauge on the heel side of the first packer shows no pressure response to injection, indicating that the isolation has been established.

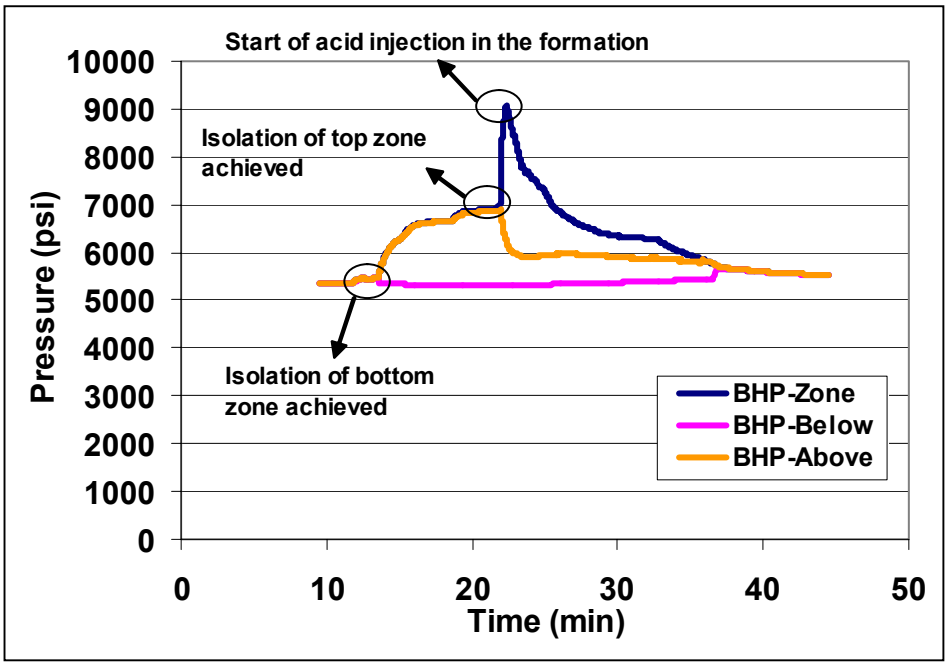

Figure 4.21 Pressure response of downhole gauges

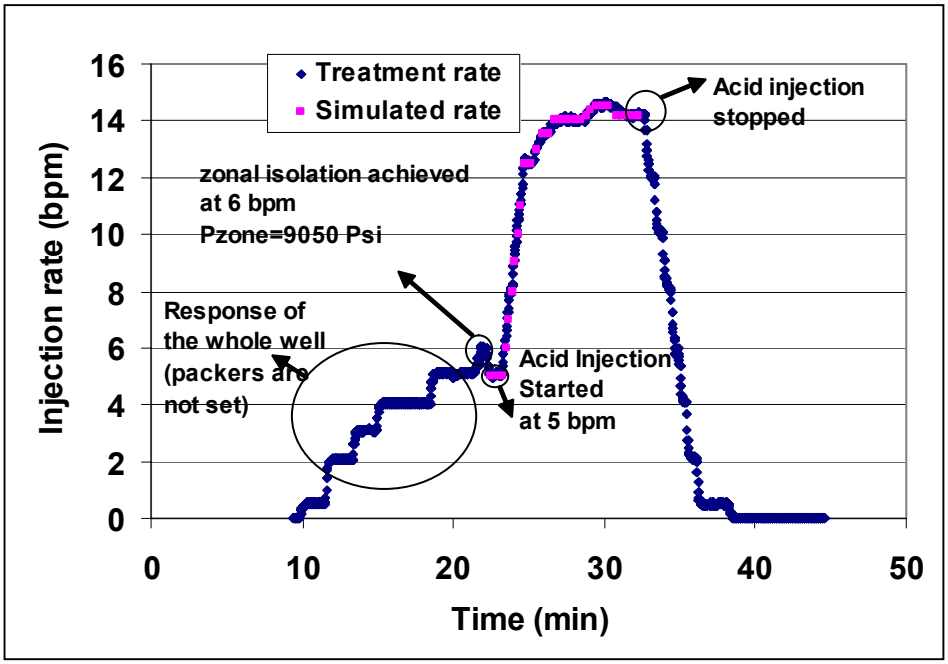

Figure 4.22 Rate schedule for North Sea field well acid treatment simulation

Then at about 22 minutes, the second packer was set, as indicated by the rapid pressure falloff recorded by the gauge beyond the second packer. It was decided to start the simulation treatment at the 22 minute, when both packers were set and acid injection into the isolated interval began. To history match the pressure response during this treatment, the actual injection rate schedule recorded is provided as input to the acid placement simulator. Fig. 4.22 shows how the approximation of the changing rate schedule as a series of discrete changing rate is done. Additional data used in the model is given in Table 4.5.

Table 4.5 Input data for North Sea field well

Casing ID	6.625 inches
Coiled tubing OD	2.55 inches
Pipe roughness	0.0001
Zone length	10 ft
Reservoir pressure in zone	5350 psi
Reservoir compressibility	5E-06 psi^{-1}
Permeability	5 md
Porosity	0.38
Initial formation damage	none
Perforation length	7 inches
Perforation diameter	0.264 inches
Perforation spacing	1 spf
Perforation phasing	0 degree
Perforation orientation	90 degree
Acid type	HCl
Acid density	69.91 lbm/ft^3
Acid viscosity	1 cp
Acid concentration	15%
Wormhole model	Volumetric
Number of grid blocks	10
Reservoir thickness	200 ft

The skin factor model is presented in Chapter II. From the data given about the well, the initial skin factor can be calculated as follows. For the given perforating conditions, a perforation skin factor of 4.6 is obtained using the Furui et al. model.[13] For this very short interval in a large reservoir, a partial penetration skin factor of -5.5 is obtained with Eq. 2.57. Combining these, and assuming no formation damage was present initially, an initial total skin factor of -0.9 is used. It is decided to adjust the reservoir permeability and the PV_{bt} in the volumetric model to obtain a match of the actual treating pressure (Fig. 4.23). This match was obtained by setting the PV_{bt} to 4.5, which means the acid is propagating wormholes relatively slowly into the matrix and that a large volume of rock is being dissolved in the treated region. With PV_{bt} of 4.5, the wormhole front is moving 4.5 times slower than the injected fluid (spent acid) front.

For the high rate injection into such a short interval, acid placement is not an issue, as shown in Fig. 4.24. What more important for this type treatment is the effects of this large volume acid treatment from the predicted depth of acid penetration into the formation. Notice that this interval has received 120 barrels of acid, about 500 gal/ft.

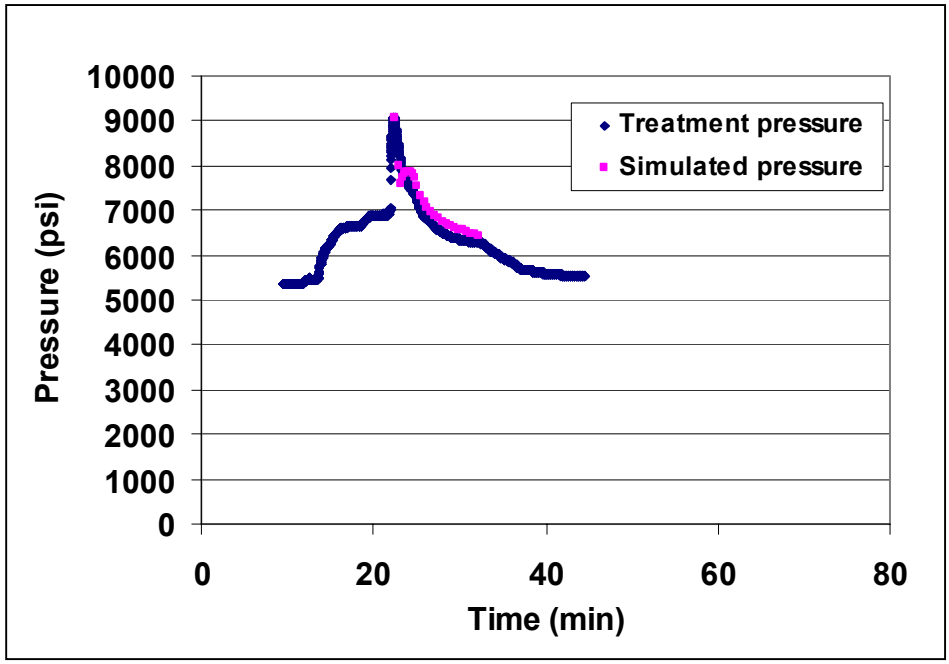

Figure 4.23 History match of treatment pressure

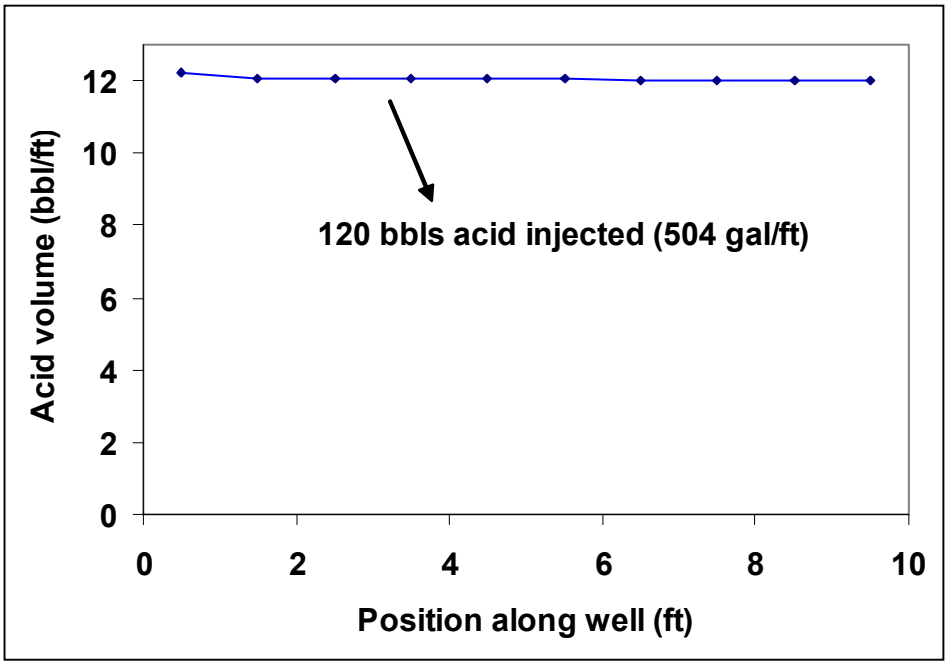

Figure 4.24 Acid placement for North Sea field well

From the history-matched pressure response using a PV_{bt} of 4.5, it can be predicted that a radial region of wormholes has propagated about 40 inches into the formation. The volumetric model presumes that the acid is dissolving a fixed fraction of rock, given by[1]

$$\eta = N_{Ac} PV_{bt} \tag{4.1}$$

Where the Acid Capacity No., N_{Ac}, is

$$N_{Ac} = \frac{\phi \beta_{15} \rho_{HCl}}{(1-\phi)\rho_{rock}} \tag{4.2}$$

For this high porosity chalk formation, η is 0.22, meaning that in the regions where wormholes have formed, 22% of the rock has been removed. With the initial porosity in this chalk formation being 38%, after this amount of dissolution, the porosity would be 0.52. It is likely that this amount of dissolution would result in the collapse of some of the remaining rock in this region, leaving a large cavern.

Based on the dissolving power of 15 % HCl reacting with calcite, 12 bbl of acid injection into a single perforation will dissolve 5.5 ft^3 of solid. Assuming that the dissolution region extends 40 inches from the wellbore, as predicted by the volumetric model with PV_{bt} = 4.5 as used in this history match, the acid has likely dissolved a sufficient amount of rock out to at least this distance to make the remaining rock unstable.

CHAPTER V

CONCLUSIONS

5.1 Conclusions

An acidizing model has been developed for horizontal wells in carbonate reservoirs, which incorporates a wellbore flow model, an interface tracking model, a wormhole model to predict the effect of the acid injection on local injectivity, a skin evolution model that combines the stimulation effect of the acid with other skin effects, and a transient reservoir inflow model. With this model, it was found that

- Small volume treatments in long horizontal intervals result in non-uniform acid placement, but that the placement improves with increasing acid volume;
- In horizontal wells completed with slotted liners, matrix acidizing might overcome the high completion skins, as wormholes pass through the flow convergence zones;
- Partial penetration effects are important when injecting into relatively short intervals of long horizontal wells;
- The parameters in a wormholing model can be adjusted to history match (or predict) the pressure response of an acid treatment in a horizontal well;
- History matching of an acid treatment in a North Sea well completed in a chalk formation required a relatively high value of the pore volumes to breakthrough parameter, suggesting that the acid is propagating slowly into the rock, creating a cavity around the wellbore.

REFERENCES

1. Economides, M. J., Hill, A. D., and Ehlig-Economides, C.: *Petroleum Production Systems*, Prentice Hall, Englewood Cliffs, NJ, 1994.

2. Rae, P. and Di Lullo, G.: "Matrix Acid Stimulation – A Review of the State-of-the-Art," paper SPE 82260 presented at the 2003 SPE European Formation Damage Conference, The Hague, 13-14 May.

3. Jones, A. T. and Davies, D. R.: "Quantifying Acid Placement: The Key to Understanding Damage Removal in Horizontal Wells," paper SPE 31146 presented at the 1996 SPE Formation Damage Control Symposium, 14-15 February, Lafayette, Louisiana.

4. Buijse, M. and Glasbergen, G.: "Improved Acid Diversion Using a Placement Simulator," paper SPE 102412 presented at 2006 SPE Russian Oil and Gas Technical Conference and Exhibition, Moscow, Russia, October 3-6.

5. Eckerfield, L. D., Zhu, D., Hill, A. D., Thomas, R. L., Robert, J. A., and Bartko, K.: "Fluid Placement Model for Horizontal-Well Stimulation," *SPE Drilling & Completions,* (September 2000) **15**, No. 3.

6. Gdanski, R.: "Recent Advances in Carbonate Stimulation," paper IPTC 10693 presented at the 2005 International Petroleum Technology Conference, 21-23 November, Doha, Qatar.

7. Bazin, B., Charbonnel, P., and Onaisi, A.: "Strategy Optimization for Matrix Treatments of Horizontal Drains in Carbonate Reservoirs, Use of Self-Gelling Acid Diverter," paper SPE 54720 presented at the 1999 SPE European Formation Damage Conference, The Hague, 31st May-1st June.

8. Mitchell, W.P., Stemberger, D., and Martin, A.N.: "Is Acid Placement Through Coiled Tubing Better Than Bullheading?," paper SPE 81731 presented at the 2003 SPE/ICoTA Coiled Tubing Conference, Houston, Texas, 8-9 April.

9. Lee, J., Rollins, J.B., and Spivey, J.P.: *Pressure Transient Testing*, SPE Textbook Series, Vol. 9, SPE, Richardson, Texas (2003).

10. Fredd, C.N., and Miller, M.J.: "Validation of Carbonate Matrix Stimulation Models," paper SPE 58713, presented at the 2000 SPE International Symposium On Formation Damage Control, Lafayette, LA, February 23-24, 2000.

11. Hill, A. D., Zhu, D., and Wang, Y.: "The Effect of Wormholing on the Fluid-Loss Coefficient in Acid Fracturing," *SPE Production and Facilities*, (November 1995) **10**, No. 4.

12. Buijse, M. and Glasbergen, G.: "A Semiempirical Model to Calculate Wormhole Growth," paper SPE 96982 presented at 2005 SPE Annual Technology Conference, Dallas, Texas, October 9-12.

13. Furui, K., Zhu, D., and Hill, A.D.: "A Comprehensive Skin-Factor Model of Horizontal-Well Completion Performance," *SPE Production and Facilities*, (August 2005) **20**, No. 3.

14. Karakas, M., and Tariq, S.M.: "Semianalytical Productivity Models for Perforated Completions, " *SPEPE* (February 1991), 73-82.

15. Muskat, M.: *Flow of Homogeneous Fluids Through Porous Media*, McGraw Hill Book Co., New York, (1937).

16. Cinco-Ley, H., Ramey, H. J., Jr., and Miller, F. G.: "Pseudoskin Factors for Partially-Penetrating Directionally-Drilled Wells," paper SPE 5589 presented at the SPE-AIME Annual Conference, Sept. 28-Oct. 1, 1975, Dallas, Texas.

17. Odeh, A. S.: "An Equation for Calculating Skin Factor Due to Restricted Entry," *JPT*, (June 1980,) 964-965.

18. Papatzacos, P.: "Aproximate Partial-Penetration Pseudoskin for Infinite-Conductivity Wells," *SPE Reservoir Engineering*, (May 1987,) 227-234.

NOMENCLATURE

a = half length of open interval, ft

a_j = parameter in inflow equation, bbl/min-psi

a_m = correlation constant for s_{2D}

A = cross-sectional area of wellbore, ft^2

A_i = coefficients in solution matrix

b_j = parameter in inflow equation, bbl/min

b_m = correlation constant for s_{wb}

B = B-function in Buijse's model

B_i = coefficients in solution matrix

c_m = correlation constant for s_{wb}

c_t = total compressibility, psi^{-1}

C_i = coefficients in solution matrix

d = internal diameter of wellbore, ft

d_m = correlation constant for s_{3D}

e_m = correlation constant for s_{3D}

f_f = fanning friction factor, dimensionless

f_m = correlation constant for s_{3D}

g_m = correlation constant for s_{3D}

h = reservoir thickness, ft

h_i = interval height (perforations), m

h_p = perforation spacing, spf

h_w = length of completed interval, ft

J = productivity index, bbl/day/psi

k = permeability of reservoir rock, md

$\mathbf{K}$ = coefficient matrix

k_{cz} = permeability of crushed zone, md

k_d = permeability of damaged region, md

$k_.$ = permeability inside slot, md

l = length of reservoir segment, ft

l_{Ds} = dimensionless slot width, dimensionless

l_p = perforation length, inches

$l_{p,eff}$ = effective perforation length, inches

l_{ps} = damage length covering over a perforation, inches

l_{pD} = dimensionless perforation length, dimensionless

l_s = slot length, inches

l_u = slot unit length, inches

L = length of wellbore, ft

m_s = num. of slot units around the circumference of the liner

m_p = num. of perforations around the circumference of the casing

n_s = num. of slots per slot unit

N_{Ac} = acid capacity number, dimensionless

N_{Re} = Reynolds number, dimensionless

O_s = Fraction of open area in a slotted liner

p_D = dimensionless pressure

$p_{R=}$ initial reservoir pressure, psi

p_w = pressure at any point in the wellbore, psi

p_{wf} = wellbore flowing pressure at heel, psi

PV_{bt} = pore volume for break through, dimensionless

$PV_{bt\text{-}opt}$ = optimum $PV_{bt,}$ dimensionless

q_i = injection rate at heel, bbl/min

q_R = reservoir inflow rate per unit length of wellbore, bbl/min/ft

q_w = wellbore flow rate at any point, bbl/min

Δq = change in rate, bbl/min

Q = volumetric flow rate (Buijse's model), m^3/s

r = radius, m

r_b = outer boundary radius, ft

r_{cz} = radius of crushed zone, ft

r_d = radius of damaged zone, ft

r_D = dimensionless radius

r_e = reservoir drainage radius, ft

r_p = perforation radius, inches

r_{pD} = dimensionless perforation radius

r_w = wellbore radius, ft

r_{wh} = radius of wormhole region, inches

s = skin factor, dimensionless

s_{pp} = partial penetration skin factor for horizontal wellbore, dimensionless

s_c = partial completion skin factor, dimensionless

s_c' = partial completion skin factor using h_w for thickness, dimensionless

s_{wb} = wellbore blockage skin factor, dimensionless

s_{2D} = 2D plane flow skin factor, dimensionless

s_{3D} = 3D convergence skin factor, dimensionless

s_p = perforation skin factor, dimensionless

s_t = total skin factor, dimensionless

t = time, minutes

t_D = dimensionless time

Δt = time step, minutes

u = average velocity,

V = volume, ft^3

V_i = interstitial fluid velocity in pores, m/s

$V_{i\text{-}opt}$ = optimum V_i , m/s

V_{wh} = velocity of wormhole front , m/s

w_s = slot width, inches

w_u = slot unit width, inches

w_{uD} = dimensionless slot width, inches

W_{eff} = constant in wormhole model, $(m/s)^{1/3}$

W_B = constant in wormhole model, $(m/s)^{-2}$

x = position of any point along the wellbore length, ft

x_{int} = location of interface from the heel of the well, ft

Δx_i = length of each grid block, ft

Z_w = elevation of completed interval, ft

α = perforation orientation, degrees

β_1 = empirical parameter for s_{3D}

β_2 = empirical parameter for s_{3D}

β_{15} = gravimetric dissolving power of 15% HCl, dimensionless

γ = dimensionless parameter for the axial convergence flow

η = wormholing efficiency, dimensionless

ξ = pressure drop function, psi/ft/bbl/min

μ = viscosity of fluid, cp

ξ = ellipsoidal coordinate dimension

ρ = density of fluid in wellbore, lb_m/ft^3

ρ_{HCl} = density of HCl, lb_m/ft^3

ρ_{rock} = density of rock, lb_m/ft^3

Φ = porosity of the reservoir rock, fraction

λ = slot (perforation) penetration ratio, dimensionless

υ = dimensionless parameter for the slot-induced radial flow, dimensionless

ε = pipe roughness, dimensionless

Subscripts

D = dimensionless

eff = effective

eq= equivalent

l= linear flow

r= radial flow*s*

SL= slotted liner

APPENDIX A

MATRIX ACIDIZING SIMULATOR

A.1 Formulation of Equations

As stated in Chapter II, in oilfield units the wellbore pressure drop equation is written in differential form as,

$$\frac{\partial p_w}{\partial x} = -1.525 f_f \frac{\rho q_w{}^2}{d^5} \tag{A.1}$$

The above equation is non-linear in nature. To make this equation linear, q_w can be separated as,

$$\frac{\partial p_w}{\partial x} = \left(\frac{-1.525 f_f \rho q_w}{d^5} \right) q_w \tag{A.2}$$

The above equation can also be written as,

$$\frac{\partial p_w}{\partial x} = \xi q_w \tag{A.3}$$

Where ξ is a coefficient defined as,

$$\xi = \frac{-1.525 f_f \rho q_w}{d^5} \tag{A.4}$$

Equation A.4 implies that the coefficient ξ is dependent on the terms q_w and f_f. f_f also depends on q_w as the friction factor is flow regime dependent i.e. laminar, transient or turbulent. In our simulator Eq. A.3 can be used as if the value of coefficient ξ is calculated at the previous time step, the nature of this equation becomes linear and it can be solved with high accuracy. This equation will be coupled with the reservoir flow equation while solving for the wellbore pressure and flow rate during the simulation of matrix acidizing process.

The reservoir flow equation as defined in Chapter II is,

$$-\frac{2\pi kl}{\mu}(p_R - p_w) = \sum_{j=1}^{n} \Delta q_j \left[p_D(t_n - t_{j-1})_D\right] + q_n s_n \tag{A.5}$$

Where:

$$\Delta q_j = q_j - q_{j-1} \tag{A.6}$$

$$t_D = \frac{4.395\times10^{-6} kt}{\phi\mu c_t {r_w}^2} \tag{A.7}$$

$$p_D \approx \frac{1}{2}(\ln t_D + 0.80907) \tag{A.8}$$

If the wellbore is divided into small segments of length *l*, then Eq. A.5 can be applied for each segment as the acid injection imitates and early radial flow pattern. The term q_R (=q/l) is specific reservoir outflow defined in unit bpm/ft. After dividing the Eq. A.5 by *l* and rearranging, we get,

$$-\frac{2\pi k}{\mu}(p_R - p_w) = \left[\sum_{j=1}^{n-1} \Delta q_{Rj} p_D(t_n - t_{j-1})_D\right] + \Delta q_{Rn} p_D(t_n - t_{n-1})_D + q_{Rn} s_n \tag{A.9}$$

The above equation can further be rearranged by using Eq. A.6 as,

$$-\frac{2\pi k}{\mu}(p_R - pw) = \left[\sum_{j=1}^{n-1} \Delta q_{Rj} p_D(t_n - t_{j-1})_D\right] - q_{Rn-1} p_D(t_n - t_{n-1})_D + q_{Rn}[p_D(t_n - t_{n-1})_D + s_n] \tag{A.10}$$

After rearranging Eq. A.10, q_{Rn}, the transient injection rate per unit length of wellbore at time t^n can be written as;

$$q_{Rn} = -a_J\left(p_R - p_w\right) - b_J \tag{A.11}$$

where coefficients a_J and b_J are defined by Eqs. A.12 and A.13 respectively,

$$a_J = \frac{4.91816\times10^{-6}\,k}{\mu[p_D(t_n - t_{n-1})_D + s_n]} \tag{A.12}$$

$$b_J = \frac{\left[\sum_{j=1}^{n-1}\Delta q_{Rj}\,p_D(t_n - t_{j-1})_D\right] - q_{Rn-1}p_D(t_n - t_{n-1})_D}{[p_D(t_n - t_{n-1})_D + s_n]} \tag{A.13}$$

The constants in Eqs. A.12 and A.13 are for oilfield units of bpm/ft for injection rate, md for permeability, and cp for viscosity.

Now the Eq. A.11, can be coupled with the wellbore material balance equation defined in Chapter II (Eq. 2.1) as,

$$\frac{\partial q_w}{\partial x} = a_J\left(p_R - p_w(t_n)\right) + b_J \tag{A.14}$$

Initial and boundary conditions to solve this system of equations are to be defined as;

$$\begin{aligned} &q_w(x,0) = 0 \\ &p_w(x,0) = p_R \\ &q_w(x,t) = 0; x \geq L \end{aligned} \tag{A.15}$$

The first and second condition explain that the initial wellbore flow rate at any point is zero (i.e. q_w=0) as the wellbore pressure is equal to the reservoir pressure (i.e. $p_w = p_{R)}$. The third condition explains that there is no lateral flow in the wellbore beyond the toe of the well (i.e. $x>L$).

Along with these initial and boundary conditions the injection rate at the heel of the well (i.e. x=0) is defined as in Eq. A.16;

$$q_w(0,t) = q_i(t) \tag{A.16}$$

A.2 Solution Matrix Construction

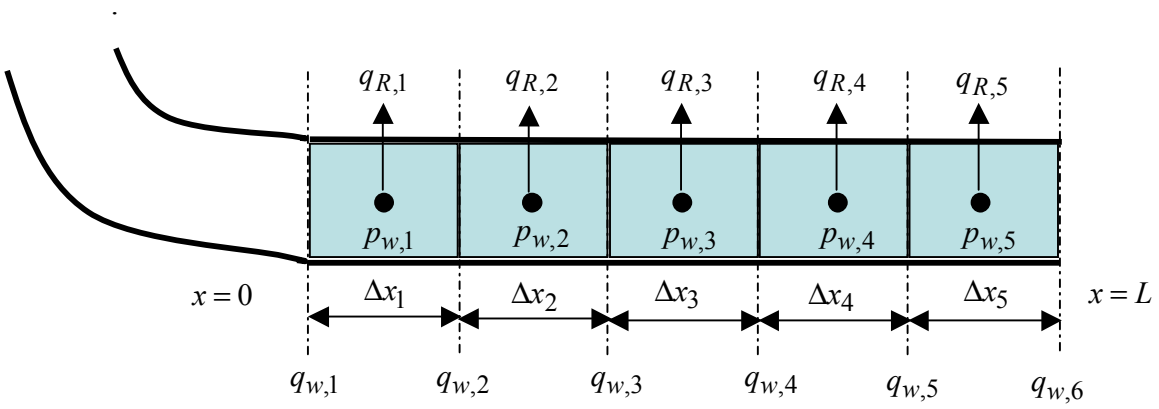

Figure A.1 A schematic of segmented wellbore

Figure A.1 provides a schematic of segmented wellbore. In this example case the whole well length; L is divided into 5 segments. The wellbore pressure in each segment is defined as $p_{w,i}$, where i denotes the segment number. These segments can be of a uniform size or a nonuniform size. Length of each segment is defined as Δx_i and specific reservoir outflow from each segment is denoted as $q_{R,i}$. The wellbore flow is defined as $q_{w\,i}$ as it is defined at the faces of the grid blocks.

The wellbore pressure drop equation i.e. Eq. A.3 can be written in discretized form as;

$$p_{w,i+1} - p_{w,i} = -\frac{(\Delta x_{i+1} + \Delta x_i)}{2} \xi_{i+1} q_{w,i+1} \qquad \text{For } i\text{=1, 2, 3, 4} \tag{A.17}$$

where the values of coefficient ξ are to be calculated from the values of q_w at the interfaces of grid blocks, obtained from previous time step.

The equation which couples wellbore material balance and reservoir flow, i.e. Eq. A.14 can be also written in discretized form as;

$$q_{w,i+1} - q_{w,i} = \Delta x_i [a_{J,i}(p_R - p_{w,i}) + b_{J,i}] \qquad \text{For } i\text{=1, 2, 3, 4, 5} \qquad \text{(A.18)}$$

where coefficients $a_{J,i}$ and $b_{J,i}$ are defined for every individual grid blocks as,

$$a_{J,i} = \frac{4.91816\times10^{-6} k}{\mu[p_D(t_n - t_{n-1})_D + s_n]} \qquad \text{(A.19)}$$

$$b_{J,i} = \frac{\left[\sum_{j=1}^{n-1} \Delta q_{Rj} p_D(t_n - t_{j-1})_D\right] - q_{Rn-1} p_D(t_n - t_{n-1})_D}{[p_D(t_n - t_{n-1})_D + s_n]} \qquad \text{(A.20)}$$

These coefficients are different for every grid block as they depend on the grid block properties such as reservoir outflow, permeability, porosity, or skin etc.

After combining the Eqs. A.17 and A.18, a set of 9 algebraic equations can be obtained for the wellbore which is divided into 5 segments. For n segments, one will have ($2n$-1) algebraic equations. After applying the initial and boundary conditions these equations reduce to a tri-diagonal matrix system as,

$$\begin{pmatrix} A_1 & 1 & 0 & 0 & 0 & 0 & 0 & 0 & 0 \\ -1 & C_2(q) & 1 & 0 & 0 & 0 & 0 & 0 & 0 \\ 0 & -1 & A_2 & 1 & 0 & 0 & 0 & 0 & 0 \\ 0 & 0 & -1 & C_3(q) & 1 & 0 & 0 & 0 & 0 \\ 0 & 0 & 0 & -1 & A_3 & 1 & 0 & 0 & 0 \\ 0 & 0 & 0 & 0 & -1 & C_4(q) & 1 & 0 & 0 \\ 0 & 0 & 0 & 0 & 0 & -1 & A_4 & 1 & 0 \\ 0 & 0 & 0 & 0 & 0 & 0 & -1 & C_5(q) & 1 \\ 0 & 0 & 0 & 0 & 0 & 0 & 0 & -1 & A_5 \end{pmatrix} \begin{pmatrix} p_{w,1} \\ q_{w,2} \\ p_{w,2} \\ q_{w,3} \\ p_{w,3} \\ q_{w,4} \\ p_{w,4} \\ q_{w,5} \\ p_{w,5} \end{pmatrix} = \begin{pmatrix} A_1 p_R + B_1 + q_i \\ 0 \\ A_2 p_R + B_2 \\ 0 \\ A_3 p_R + B_3 \\ 0 \\ A_4 p_R + B_4 \\ 0 \\ A_5 p_R + B_5 \end{pmatrix} \qquad \text{(A.21)}$$

The coefficients of the matrix A, B, and C are defined by Eqs. A.22, A.23, and A.24 respectively.

$$A_i = \Delta x_i a_{J,i} \tag{A.22}$$

$$B_i = \Delta x_i b_{J,i} \tag{A.23}$$

$$C_i = (\Delta x_i + \Delta x_{i-1})\xi_i / 2 \tag{A.24}$$

The coefficient C_i contains the term ξ_i which depends on the wellbore flow rate defined at the grid block interfaces. These equations are nonlinear in nature and solution is obtained by solving equations successively in time so that the coefficients ξ_i , and thus C_i, are calculated using the wellbore flow rate values from the last time step. The system of equations defined in Eq. A.21 can also be written as;

$$\mathbf{K}(q) \times \mathbf{u} = \mathbf{f} \tag{A.25}$$

The vector **K** in above equation is coefficient matrix i.e. left most matrix in Eq. A.21. **f** is a vector denoted by right hand side matrix in Eq. A.21. **u** is solution vector and it is the matrix which is in middle of Eq. A.21. The matrix defined by Eq. A.21 is a tri-diagonal matrix system, which is a system of nonlinear algebraic equations. The pressure values at the heel (i.e. $p_{w,1}$) are to be achieved by solving this matrix system. Consider first the case where the coefficient matrix is not a function of the flux distribution. In this case, Eq. A.21 reduces to a linear matrix problem, which can be solved directly, without iteration, by the standard matrix methods. In second case where the coefficient matrix is a function of function of flux distribution, then Eq. A.21 becomes nonlinear and it should be linearized first. A simple successive substitution iteration scheme is applied as follows;

$$\mathbf{K}(q^k)\mathbf{u}^{k+1} = \mathbf{f} \tag{A.26}$$

Where superscript *k* denotes the iteration number, **u** is a solution vector, and **f** is the right hand side vector as defined in Eq. A.21. The injection rate varies with time, and solution of the system of equations will then provide the pressure variation at the heel with time i.e. $p_w(0,t)$. The solution scheme to solve these equations is explained in the separate section.

A.3 Simulator Flow Chart

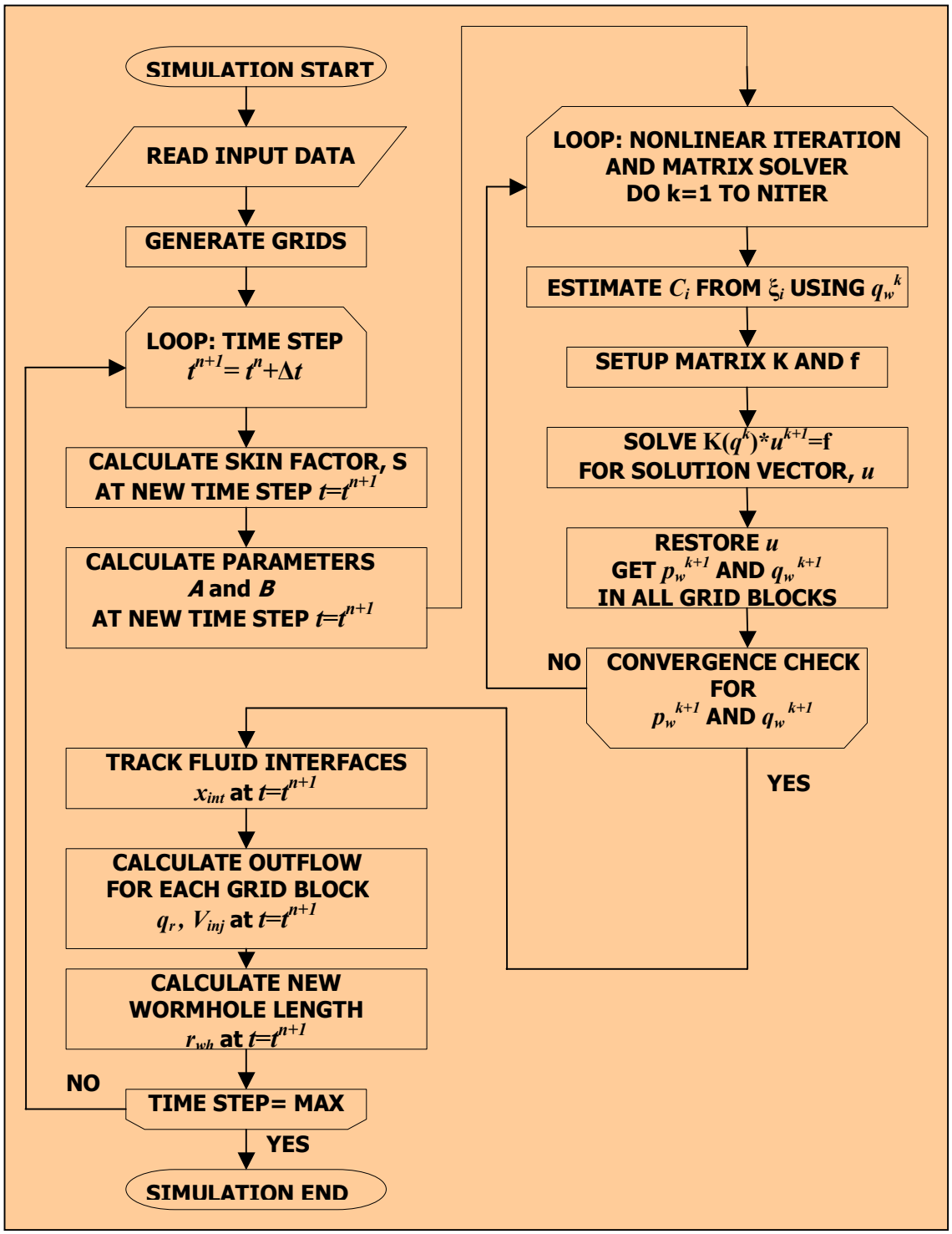

Figure A.2 A flow chart for matrix acidizing simulator

The flow chart for the acidizing simulator is shown in Fig. A.2. The overall time of injection is divided into small time steps and this solution matrix is solved for each time step considering the injection rate schedule defined at heel. The wellbore length is divided into various segments, and this is provided to simulator as input. The program generates the grids and defines the individual grid block length and position from the heel of the well. At a new time step, for every grid block new skin factors are calculated using the skin models described in Chapter II. The productivity index parameters (A_i, B_i) are then estimated at new time step using Eqs. A.22 and A.23. The solution is then obtained by performing the calculation in nonlinear iteration loop. The simulator estimates the coefficients C_i using Eq. A.24, which is dependent on frictional pressure drop parameter ξ_i. This parameter ξ_i is a function of q_w i.e. the wellbore flow rate. The initial conditions indicate that the initial wellbore pressure is equal to the wellbore pressure and there is no flow in the wellbore. The matrix defined in Eq. A.21 is solved after defining the parameters of the right hand side vector as well as of the coefficient matrix. A convergence check allows the simulator to check that the values of the solution vector (flow rates at grid block interfaces and pressures in grid blocks), i.e. the difference in the values of solution vector between two nonlinear iterations, are converging or not. If the solution of the Eq. A.21 converges then the process comes out from the nonlinear iteration loop and the pressure values at the heel can be obtained from this solution i.e. $p_{w,1}$.

Once the iterations for the convergence check are complete, the simulator estimates the fluid interface movement using the Eq. 2.14 described in Chapter II. Once the new location of fluid interfaces are calculated and stored in the memory, the simulator estimates the outflow for each grid. This information has been fed into wormhole model to estimate the wormhole growth at the end of the time step. Wormhole models are described in Chapter II. Two types of wormhole models are incorporated into the simulator, volumetric wormhole model, and the Buijse model.

The skin for each grid block is to be calculated at new time step with using the new wormhole length. Skin models for various completions are presented in Chapter II. This new skin factor is used in estimating the productivity index parameters i.e. a_J and b_J. The

same process for nonlinear iterations is repeated using the initial values of q_w^k from the last solution vector **u**.

The simulation ends when the time step reaches to the end. The output from the simulator gives the pressure values at the heel ($p_{wf} = p_{w,1}$) for each time step. The bottomhole pressure is a valuable information needed to evaluate the performance of acidizing process. For a particular injection rate schedule these values are obtained from the acid placement simulator. A history match can then be performed for observed pressure and simulated pressure by varying the treatment and well parameters.

APPENDIX B

MATRIX ACIDIZING SIMULATOR INPUT DATA FILE

```
---INPUT DATA FILE FOR MATRIX ACIDIZING SIMULATOR
---WELL CONFIGURATIONS AND RESERVOIR PROPERTIES
--KEYWORD (%WRC) FORMAT
--LINE 1- [WELLBORE OD (IN)] [CASING ID (IN)] [TUBING OD (IN)] [PIPE ROUGHNESS]
--LINE 2- [WELLBORE LENGTH (FT)] [TUBING TAIL LOCATION, =0 FOR HEEL (FT)] [CT (1/PSI)] [PARTIAL PENETRATION SKIN]
--LINE 3- [RESERVOIR PRESSURE, PR, PSI] [INITIAL PRESSURE IN TUBING, PINI, PSI] ENTER PR=PI IF INITIAL CONDITION IS SAME
--LINE 4- [INITIAL RATE, QI BBL/DAY ENTER 0 IF PR=PI]
--LINE 5- [TVD] [MD] [TUBING TYPE]
--LINE 6- [ROCKTYPE-LIMESTONE OR DOLOMITE] [ROCK DENSITY (G/CM3)]
--LINE 7- [NO OF GRIDS]
--LINE 8- [COMPLETION TYPE, OPENHOLE-OH, CASED-PERFORATED-CP, SLOTTED LINER-SL]
--FROM LINE 9 ONWARDS TO (NUMBER OF GRIDS)
--FOR OPENHOLE COMPLETION
-- [GRID NO.] [STATUS, OPEN/CLOSE] [DX (FT)] [ANI] [PORO (FRAC)] [KH (MD)] [RKS (KD/K)] [RS (FT)]
--FOR CASED-PERFORATED COMPLETION
-- [GRID NO.] [STATUS, OPEN/CLOSE] [DX (FT)] [ANI] [PORO (FRAC)] [KH (MD)] [RKS (KD/K)] [RS (FT)] [MP] [LP (IN)] [DP (IN)] [NP (SPF)] [ALPHA (DEGREE)] [RKCZ] [DCZ (IN)]
%WRC
6.625     6.625     2.875     0.0001
1000      0         1. 7E-05            0
3200
0
10557     14900     2
LIMESTONE      2.71
10
CP
1    OPEN    100    1    0.38    2    0.5    1    2    9    0.3    1    90    1    0.0003
2    OPEN    100    1    0.38    2    0.5    1    2    9    0.3    1    90    1    0.0003
3    OPEN    100    1    0.38    2    0.5    1    2    9    0.3    1    90    1    0.0003
4    OPEN    100    1    0.38    2    0.5    1    2    9    0.3    1    90    1    0.0003
5    OPEN    100    1    0.38    2    0.5    1    2    9    0.3    1    90    1    0.0003
```

6 OPEN 100 1 0.38 2 0.5 1 2 9 0.3 1 90 1 0.0003

7 OPEN 100 1 0.38 2 0.5 1 2 9 0.3 1 90 1 0.0003

8 OPEN 100 1 0.38 2 0.5 1 2 9 0.3 1 90 1 0.0003

9 OPEN 100 1 0.38 2 0.5 1 2 9 0.3 1 90 1 0.0003

10 OPEN 100 1 0.38 2 0.5 1 2 9 0.3 1 90 1 0.0003

--INJECTION SCHEDULE

--KEYWORD (%INJ) FORMAT

--LINE 1- [NUMBER OF STEPS]

--LINE 2- [BOUNDARY CONDITION TYPE, CONSTANT RATE-Q, CONSTANTE PRESSURE-P]

--LINE 3 ONWARDS TO NUMBER OF STEPS

-- [STEP NUMBER] [DURATION (MIN.)] [RATE IN BPM FOR CONSTANTE RATE OR PRESSURE IN PSI FOR CONSTANT PRESSURE)] [INJECTED FLUID TYPE SELECT FROM %IFP TABLE]

%INJ

5

Q

1 10 2 2

2 10 2 2

3 30 2 2

4 40 2 2

5 20 2 2

--INJECTED FLUID TABLE

--KEYWORD (%IFP) FORMAT

--LINE 1- [NUMBER OF FLUID TYPES]

--LINE 2 ONWARDS TO NUMBER OF FLUID TYPES AND FLUID NAME IN THE LINE ABOVE THE FLUID INFORMATION LINE

-- [FLUID NUMBER] [FLUID DENSITY(LBM/FT3)] [FLUID VISCOSITY(CP)] [CONCENTRATION OF HCL(%)] [DISSOLVING POWER]

%IFP

2

COMPLETION FLUID

1 64.29 1 0 0

ACID

2 67.4 0.5 15 1.37

--WORMHOLE MODEL

--KEYWORD (%WHM FORMAT)

--LINE 1- [WORMHOLE MODEL TYPE, 1: VOLUMETRIC, 2: BUIJSE'S MODEL]

--LINE 2- [PVBT FOR VOLUMETRIC MODEL E.G. 2, PVBT-OPT FOR BUIJSE'S MODEL E.G. 1.5]

--LINE 3- [VI-OPT FOR BUIJSE'S MODEL E.G. 0.1 CM/MIN]

%WHM

1

4.5

%END

VITA

Name:	Varun Mishra
Address:	10/220 Gandhi-Nagar Rura, Kanpur-Dehat Uttar-Pradesh, India-209303
Email Address:	varun.mishra@pe.tamu.edu
Education:	B.Tech., Petroleum Engineering, Indian School of Mines, Dhanbad, 2002
Employment History:	Oil and Natural Gas Corporation Ltd., India, From 2002 to 2005.

This thesis was typed by the author.